Tunnelling and Underground Space Technology 177 (2026) 107867

Contents lists available at ScienceDirect

Tunnelling and Underground Space Technology incorporating Trenchless Technology Research

journal homepage: www.elsevier.com/locate/tust

A comprehensive review of advanced laser scanning techniques for deformation monitoring and defect detection in shield tunnels

Shihan Fu [a], Yueqian Shen [a,*], Jinhu Wang [b], Jundi Jiang [a], Junjun Huang [a]

[a] School of Earth Sciences and Engineering, Hohai University, Nanjing 211100, China
[b] Institute for Biodiversity and Ecosystem Dynamics (IBED), University of Amsterdam, Amsterdam 1012 WX, the Netherlands

ARTICLE INFO

Keywords:
Laser scanning technology
Tunnel deformation monitoring
Point cloud processing
Defect detection

ABSTRACT

Ensuring the structural safety of shield tunnels is critical to the reliability and efficiency of modern urban transportation systems. Laser scanning (LS) has emerged as a transformative technology for tunnel deformation monitoring and defect detection because it enables rapid, non-contact acquisition of high-resolution three-dimensional point cloud data. This review provides a comprehensive analysis of LS techniques for deformation monitoring and defect detection in shield tunnels with their principles and advancements. Although LS provides detailed geometric information with high measurement accuracy, challenges remain in large-scale data processing, noise reduction, and precise registration. Moreover, the integration of LS with complementary sensors is explored to address the limitations of single-sensor systems while improving data completeness and reliability. Recent advances in defect detection, classification, and severity assessment are reviewed, highlighting their potential to support predictive maintenance and risk mitigation strategies. Finally, this review highlights current gaps and future directions to advance the application of LS technology in tunnel monitoring and enhance the safety and stability of underground infrastructure.

1. Introduction

Subway systems constitute a fundamental component of modern urban transportation, where shield tunnels represent one of the most common structural forms used in subway construction. Shield tunnels are prone to structural deformation during long-term service due to a range of external and internal stresses, as well as geological influences such as heterogeneous soil composition and water table fluctuations (Cui et al., 2024b). Additionally, operational factors including train-induced vibrations, thermal expansion and contraction, accelerate the degradation of tunnel components. Traditional monitoring techniques, including manual inspections, have been used for assessing tunnel deformation and structural condition. However, these methods are constrained by several limitations, including the lack of real-time monitoring capability and limited spatial resolution. As a result, they hinder early-stage defect detection and limit the effectiveness of preventive maintenance strategies.

Laser scanning (LS) technology has emerged as a powerful tool for the structural health monitoring (SHM) of shield tunnels (Chen et al., 2025; Lai et al., 2025). LS operates by emitting laser pulses toward the tunnel surface and measuring their time-of-flight (TOF) to acquire dense three-dimensional point cloud data. Its capability to capture high-resolution spatial information is critical for identifying subtle deformations, including misalignments, geometric deviations, and incipient cracks or defects. However, applying LS in shield tunnel monitoring remains challenging due to the complex underground environment, where limited accessibility, dust, moisture, and unstable lighting conditions can degrade data accuracy and completeness (Lai et al., 2025). Furthermore, LS systems generate large volumes of point cloud data, which require advanced algorithms and significant computational resources to process. Another critical issue lies in the integration of LS data with other monitoring technologies to achieve more comprehensive and reliable tunnel assessments.

Existing reviews has extensively explored LS in tunnel monitoring from different perspectives, focusing on fundamental surveying principles (Mukupa et al., 2017; Shen et al., 2023), early-stage engineering applications (Liu et al., 2023a), or specific image-based defect detection (Attard et al., 2018; Kuang et al., 2022). However, these reviews primarily focused on static TLS workflows or basic 2D projection-based analysis, which do not fully reflect the recent shift from geometry-only toward intelligence-driven interpretation in LS, including foundation models for 3D point clouds and end-to-end autonomous diagnostic

* Corresponding author at: School of Earth Sciences and Engineering, Hohai University, Nanjing 211100, China.
E-mail address: y.shen_lidar@hhu.edu.cn (Y. Shen).

https://doi.org/10.1016/j.tust.2026.107867
Received 7 January 2026; Received in revised form 10 April 2026; Accepted 7 June 2026
Available online 30 June 2026
0886-7798/© 2026 Published by Elsevier Ltd.

frameworks. This review distinguishes itself by providing a comprehensive and in-depth analysis of these emerging data-driven paradigms, specifically emphasizing the technical bottlenecks of deformation monitoring and defect detection using point cloud data.

Specifically, this review begins with an introduction to the fundamental principles of LS and the procedures for spatial data acquisition and analysis. Then, key system parameters, including accuracy, resolution, and point density are discussed, along with their influence on the reliability of tunnel monitoring. The main applications of LS in tunnel management are summarized, covering inspection, maintenance, and emergency response. Subsequently, the review highlights recent progress in hardware design, data-processing algorithms, and multi-sensor integration, which has improved the performance and adaptability of LS in complex underground environments. In addition, this review categorizes key challenges in applying LS to shield tunnel monitoring, including the need for robust and scalable data-processing algorithms, effective mitigation of environmental interference, and standardized frameworks for integrating LS data into management systems. Finally, the review outlines future research directions for improving the application of LS in tunnel monitoring, with an emphasis on enhancing the safety, reliability, and efficiency of subway systems. By clarifying the current capabilities and limitations of LS, this study aims to support further advancements in infrastructure monitoring and promote the sustainable development of urban transportation systems.

2. Scientometric analysis of selected papers

2.1. Literature searching and screening

Relevant literature was retrieved from the Web of Science Core Collection and Google scholar databases. The search was conducted using the keywords “laser scanning”, “shield tunnel”, “deformation monitoring”, and “defect detection” for the period from 2012 to 2026. After removing duplicates, conference abstracts, and irrelevant studies, a total of 140 papers were selected for further analysis.

2.2. Interannual distribution of literature

As shown in Fig. 1, the annual distribution of publications from 2012 to 2026 reveals an overall upward trend. From 2012 to 2017, the research field remained at an initial development stage, with a relatively small and stable number of annual publications. Specifically, only 2 papers were published in 2012, followed by a moderate increase to 7 papers in both 2013 and 2014. A slight fluctuation was observed in 2015, 2016, and 2017, reflecting the nascent and exploratory nature of the research during this phase.

The number of publications surged to 12 in 2018 and continued to climb to 14 in 2019. A slight dip occurred with 8 publications in 2020. From 2021 to 2025, the field entered its most active phase, maintaining a relatively high level of output with 17, 16, 12, 18, and 11 publications, respectively. In the first half of 2026, at least four studies closely related to tunnel monitoring have been published, indicating sustained research interest in this field.

2.3. Analysis of keywords co-occurrence

Fig. 2 illustrates the keyword co-occurrence network generated by VOSviewer, representing the main research themes and their interrelationships in the field during the period of rapid expansion after 2018. “Terrestrial laser scanning” and “point cloud” appear as the most dominant and central keywords, indicating the pivotal role of laser scanning point cloud data in tunnel-related investigations. Closely associated terms such as “laser scanning technology” and “extraction method” form the core research clusters, reflecting the methodological foundations of this domain. Keywords like “tunnel structure”, “deformation monitoring”, “registration”, and “inspection” suggest an emphasis on structural analysis and health monitoring applications.



Fig. 1. Number of literatures and trends of tunnel deformation monitoring and defect detection.

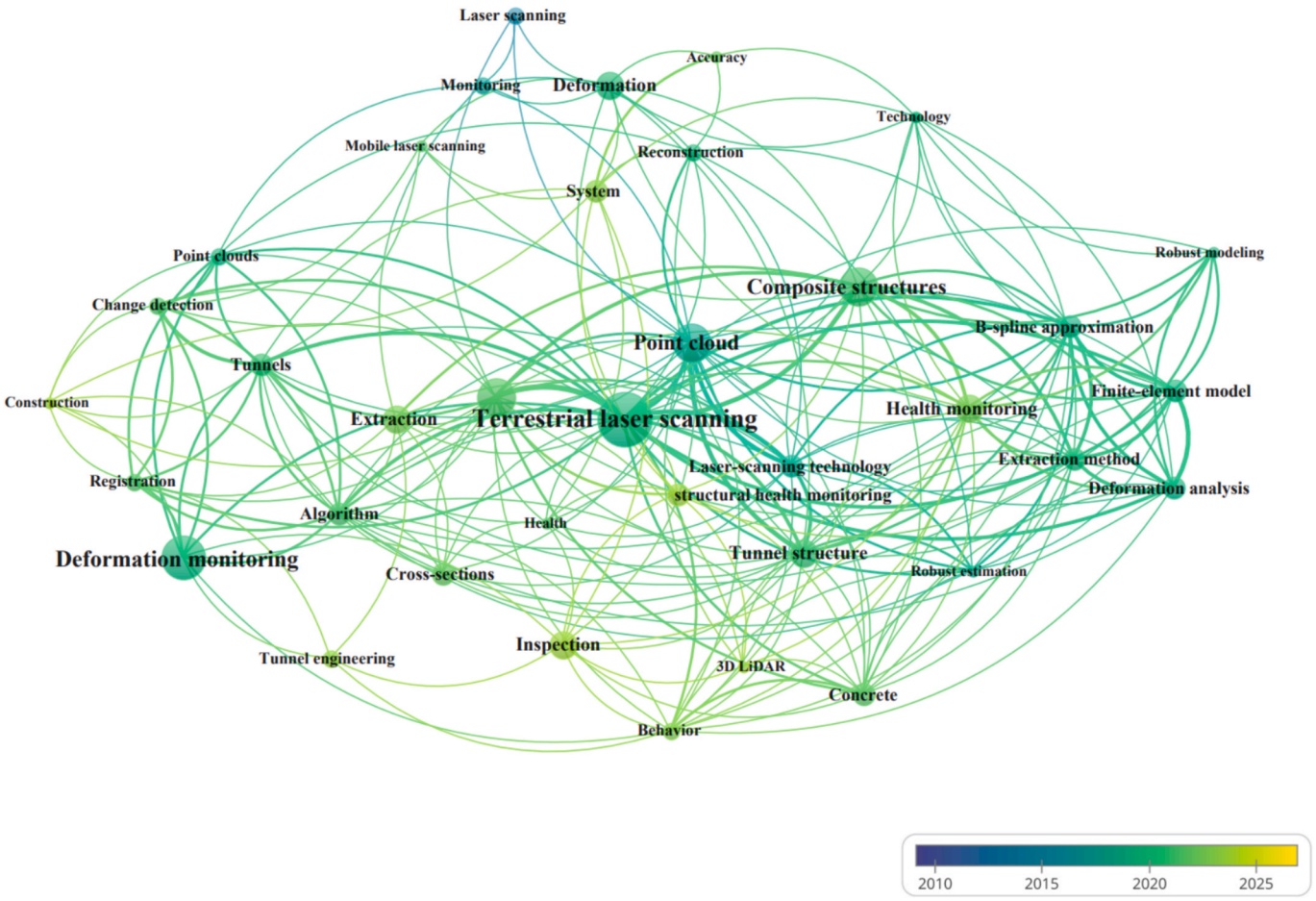


Fig. 2. Network of keyword co-occurrence.

3. Overview of laser scanning technology

3.1. Principles of laser scanning technology

Laser scanning is a remote sensing technique that measures distances by emitting laser beams toward objects and capturing the returning signals with photoelectric detectors. Depending on the underlying distance measurement principle, LS systems are generally classified into two main categories: time-of-flight based systems and phase-based systems.

As illustrated in Fig. 3(a), a time-of-flight-based laser scanning system determines the distance between the scanner and the target surface by recording the travel time of laser pulses emitted from the source, reflected by the target, and detected upon their return. The measured travel time is then converted into distance using the following equation:

$$d = \frac{c \times \Delta t}{2} \tag{1}$$

where d represents the distance, c denotes the speed of light, and Δt is the total time for the emitted light to travel to target and return.

In contrast, a phase-based laser scanning system employs a continuous-wave laser modulated by a sinusoidal signal to determine distances, as illustrated in Fig. 3(b). The system calculates the distance to a target by measuring the phase shift between the emitted and reflected signals. Since the phase shift is proportional to the distance traveled by the laser beam, the distance can be calculated using the

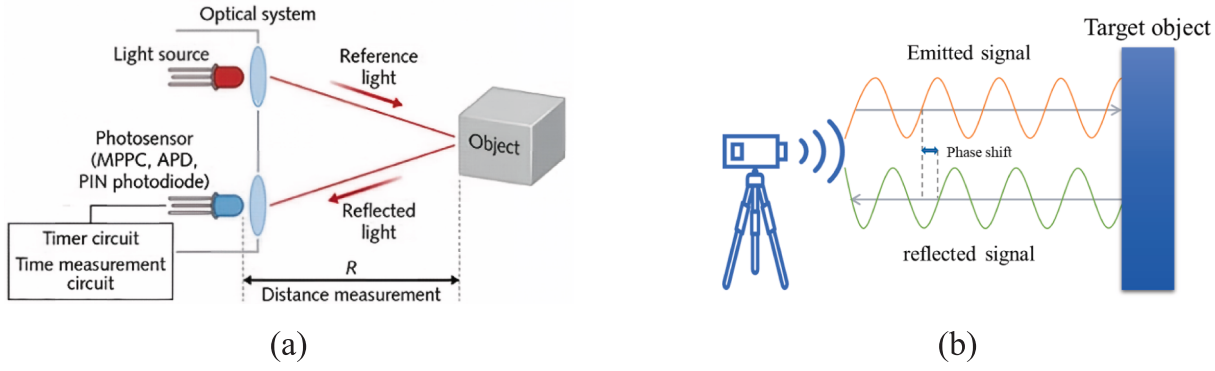


Fig. 3. Schematic diagrams of laser ranging principles: (a) time-of-flight (ToF) method (Liu et al., 2018); (b) phase-based method.

following equation:

$$D = \frac{\varphi}{4\pi} \times \lambda \tag{2}$$

where φ is the measured phase shift and λ is the modulation wavelength.

3.2. Different laser scanning systems: advantages and challenges

Laser scanning systems are typically categorized into four primary types: terrestrial, mobile, airborne, and spaceborne. The core component of laser scanning systems is the laser scanner. Some modern LS systems, particularly mobile laser scanning (MLS) systems, are also equipped with Global Navigation Satellite System (GNSS), Inertial Navigation System (INS), and RGB camera (Di Stefano et al., 2021; Williams et al., 2013; Yu et al., 2014). The laser scanner measures the distances between itself and the scanned objects, enabling the generation of detailed 3D point cloud data with high accuracy. The GNSS module provides accurate spatial positioning, which is essential for georeferencing the acquired point clouds. The INS complements this by recording orientation parameters, such as roll, pitch, and yaw angles, to correct the positioning of the scanner in dynamic environments. Additionally, the RGB camera captures true-color imagery, enriching the 3D data with color context, which is particularly valuable for applications where visual detail is required (Guan et al., 2016).

In enclosed underground environments, such as shield tunnels, airborne laser scanning systems (ALS) and spaceborne laser scanning systems (SLS) are typically unsuitable due to GNSS signal occlusion and restricted spatial conditions, which limit their operational effectiveness. In contrast, terrestrial laser scanning (TLS) and MLS systems demonstrate excellent adaptability in such confined underground spaces, as shown in Fig. 4. The following subsections provide a detailed examination of TLS and MLS, outlining their respective advantages and associated challenges in tunnel inspection applications.

3.2.1. Terrestrial laser scanning systems

TLS technology has found widespread application in diverse fields, including shield tunnel deformation monitoring (Wang et al., 2014), bridge structure assessments (Rashidi et al., 2020), and wall defect detection (Jiang et al., 2018). TLS systems are typically mounted on stationary tripods during data acquisition, as depicted in Fig. 4(a). Multiple targets are often used to achieve accurate alignment across different scanning stations. After data collection, the point clouds acquired from different stations are registered using the coordinates of these targets, leading to a unified dataset. One notable advantage of TLS is its ability to generate point clouds with high density and accuracy, making it particularly well-suited for detailed scanning in confined space. Several commonly used TLS systems are listed in Table 1.

Despite its advantages, several challenges limit the broader application of TLS. A primary constraint is the need for frequent scanner repositioning to ensure full spatial coverage in large-scale environments, which is labor-intensive and time-consuming, thereby reducing survey efficiency. Furthermore, the accuracy of the resulting point clouds depends on multi-station registration, which can be compromised by misalignment or reference target instability. External environmental factors, such as wind-induced vibrations on the tripod, can also degrade data quality and lead to measurement inaccuracies or point cloud artifacts.

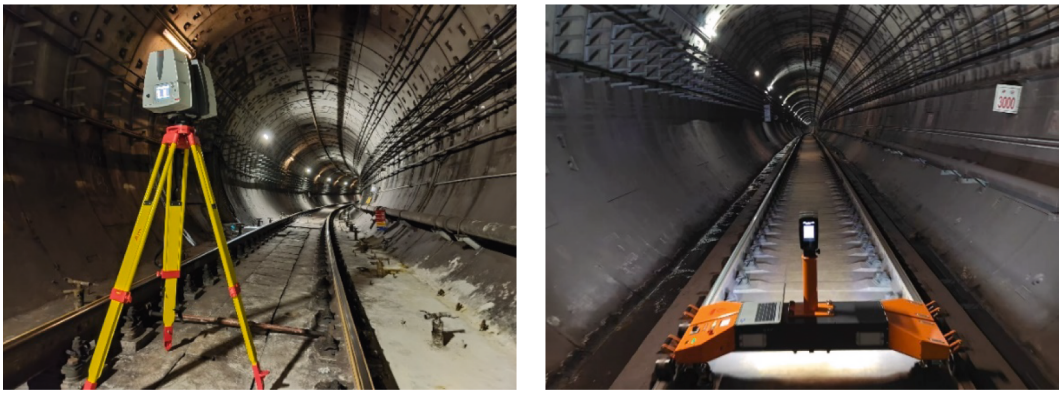
3.2.2. Mobile laser scanning systems

The MLS components, illustrated in Fig. 5, are typically mounted on various mobile platforms, such as vehicles, trolleys, boats, backpacks, or robots. This configuration allows for dynamic scanning of environments at a fixed speed, enabling efficient and rapid acquisition of point cloud data. MLS systems offer significant advantages in terms of mobility, extensive scanning coverage, and the ability to acquire high-precision and high-density point cloud data. These advantages make MLS technology particularly well-suited for capturing linear objects such as roads, railways, and tunnels, leading to its widespread application across various areas, including shield tunnel leakage detection (Huang et al., 2020; Liu et al., 2022a), powerline inspection (Shokri et al., 2021; Xu and Wang, 2019), and urban planning (Balado et al., 2018; Tang et al., 2023).

Despite these advantages, the effectiveness of MLS is affected by several factors. In underground scenarios such as tunnels, where GNSS signals are weak or unavailable, MLS must rely on alternative localization methods, including IMU-based navigation or Simultaneous Localization and Mapping (SLAM) algorithms (Taheri et al., 2021). In addition, MLS performance is influenced by the distance between the scanner and the target surface and the trajectory of the mobile platform. As the scanning distance increases, the resulting point cloud becomes sparser, reducing the level of detail in the representation of object features (Shen et al., 2024). This limitation poses challenges in applications requiring high-resolution data, especially in environments where precise feature extraction is critical.

3.3. Laser scanning systems for shield tunnel monitoring

Laser scanning systems play a pivotal role in shield tunnel monitoring by providing high-precision, detailed three-dimensional point clouds for structural analysis and deformation monitoring. In this context, TLS and MLS represent two complementary approaches, striking a balance between data accuracy and operational efficiency. Although both are widely deployed in GNSS-denied underground environments, disparities in their underlying data acquisition mechanisms



(a) (b)

Fig. 4. Scanning systems used for shield tunnel monitoring. (a) TLS. (b) MLS.

Table 1
Specifications of commonly used terrestrial laser scanners.

Device	Type	Range	Accuracy	Scan Rate (kpts/s)	Field of View (FOV: V × H)	Reference
Z + F IMAGER 5010X	TLS	187 m	0.8 mm @ 50 m	$\geq 1 \times 10^3$	320°×360°	Hu et al. (2023)
Leica RTC360	TLS	130 m	1 mm + 10 ppm	2×10^3	100° ×360°	Bauer and Woschitz (2024)
Faro Focus 350	TLS	307 m 614 m	0.2–0.3 mm @ 5 m	976 (at 307 m) 122–488 (at 614 m)	300°×360°	Xu et al. (2022)

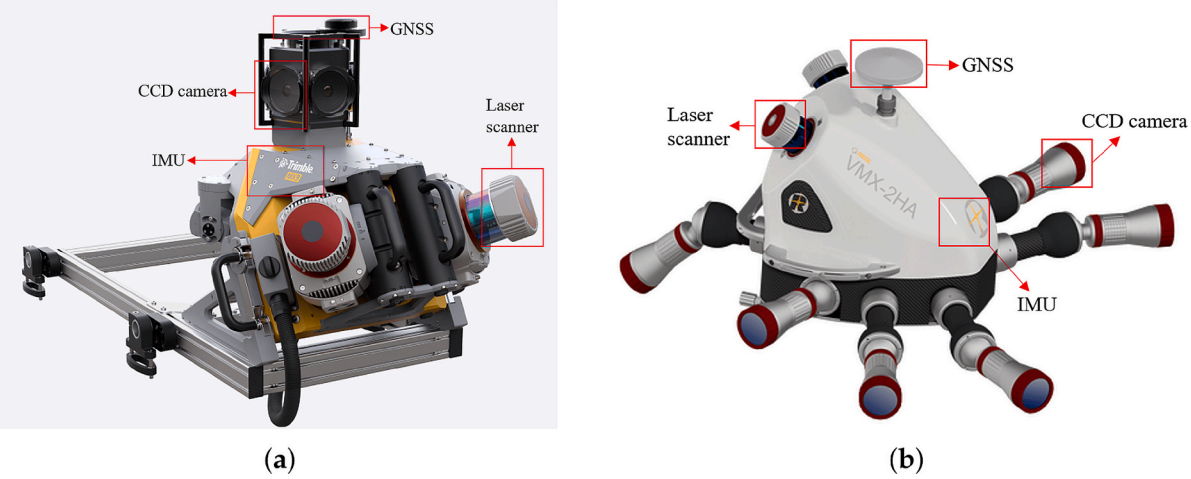


Fig. 5. Components of MLS systems: (a) Trimble MX-9. (b) RIEGL VMX-2HA (Ma et al., 2018).

result in distinct performance characteristics. TLS acquires point clouds from fixed stations by scanning the surrounding tunnel surfaces over a wide horizontal and vertical field of view. Each station captures 3D coordinates relative to the local instrument center. Multi-station scans are subsequently registered into a common coordinate system to generate a unified point cloud representing the entire surveyed area, such as a full tunnel geometry. This approach provides millimeter-level precision and is indispensable for rigorous structural deformation analysis. However, TLS is inherently limited by the spatial discretization of scan stations. When stations are positioned at excessive intervals, the resulting laser incidence angle becomes overly steep, which may diminish signal strength, reduce point cloud accuracy, and cause data occlusion. Additionally, the point cloud density exhibits a characteristic decay with increasing range.

In contrast, MLS employs a line-scan mode, as depicted in Fig. 6, whereby cross-sectional profiles are continuously acquired as the system traverses the tunnel along its longitudinal axis. This dynamic acquisition paradigm ensures relatively uniform point cloud density and superior coverage efficiency. Several MLS systems have been customized for shield tunnel applications, including CNU-TS-2 (Sun et al., 2020a), TMMS (Sun et al., 2020b), SDMLS (Xu et al., 2022), and GRP5000

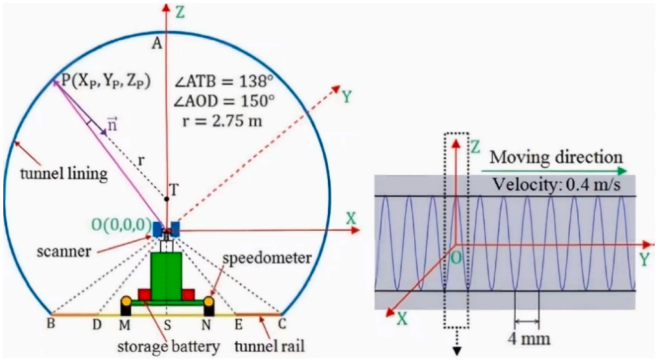


Fig. 6. Scanning mode for MLS A (Tan et al., 2016).

(Huang et al., 2020), as illustrated in Fig. 7. These systems offer significant advantages in terms of operational efficiency, making them particularly well-suited for large-scale shield tunnel deformation monitoring and defect detection. Nevertheless, this mode is susceptible to trajectory-induced drift and typically yields lower positioning accuracy relative to the static constraints of TLS.

Overall, TLS and MLS exhibit complementary characteristics: TLS provides superior accuracy at the cost of intensive manual labor, while MLS enables rapid data acquisition with a slight compromise in local precision. TLS is optimally deployed for establishing geodetic baselines and performing localized, high-resolution structural diagnostics. In contrast, MLS offers a robust solution for routine maintenance, large-scale defect detection, and geometric modeling of large-scale 3D digital twins (DT) (Zhu et al., 2025). A systematic comparison of their advantages, limitations, and applicability in diverse tunnel monitoring scenarios is summarized in Table 2. Detailed task-specific performance benchmarks are further discussed in subsequent sections.

4. Deformation monitoring in shield tunnels using laser scanning point cloud

This section provides a comprehensive review of methodologies for monitoring shield tunnel deformation using laser scanning point clouds. The general metrological workflow is conceptualized as a cohesive pipeline from raw data acquisition to high-precision deformation quantification, as systematically illustrated in Fig. 8.

The following subsections review the critical stages of this processing chain, including point cloud registration, scanning optimization, centerline extraction, cross-section analysis, and seam dislocation detection. Special emphasis is placed on the evolution of algorithms and state-of-the-art (SOTA) advances at each stage.

4.1. Registration of point clouds from adjacent stations

In shield tunnel applications, TLS is typically carried out from multiple static stations to obtain complete coverage of the tunnel interior.

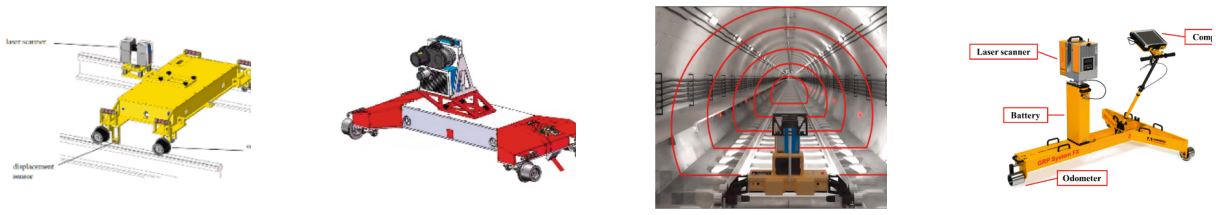


Fig. 7. Scanning mode for MLS. (a) CNU-TS-2 (Sun et al., 2020a). (b) TMMS (Sun et al., 2020b). (c) SDMLS (Xu et al., 2022). (d) GRP5000 (Huang et al., 2020).

Table 2
Comparative analysis of metrological attributes and operational suitability for typical tunnel laser scanning systems.

System	Scanning Mode	Key Advantages	Limitations	Optimal application
TLS	– Static; – Multi-station setup.	– Millimetric precision; – High point density; – Reliable for fine-grained details.	– Low efficiency due to manual station-setting; – Occlusion effects in complex zones.	– High-precision deformation analysis; – Defect detection; – Baseline survey.
MLS	– Mobile; – Vehicle-mounted.	– High-speed and efficiency; – Continuous data acquisition; – Large coverage.	– Precision heavily dependent on trajectory accuracy; – Lower point density than TLS.	– Rapid inventory of long-distance tunnels; – Large-scale structural inspection; – 3D digital twinning.

The point clouds acquired at these stations must be registered into a common coordinate system to enable reliable deformation monitoring. However, the registration of point cloud data from multiple stations will inevitably introduce positional and transformation errors. This issue becomes particularly significant in long and linear structures such as shield tunnels, where even minor errors can accumulate and magnify along the tunnel length. This cumulative effect, commonly referred to as error propagation, poses a significant challenge to maintaining the overall geometric fidelity and spatial accuracy of the reconstructed tunnel model. If unmitigated, these errors can severely compromise the precision of subsequent deformation analysis and structural assessments.

To address these challenges, various methods have been developed for registering adjacent station point clouds in tunnel environments. The primary categories of these methods are summarized and discussed below:

(1) Geometric feature-based registration methods

Geometric feature-based registration methods align point clouds acquired from different scanning stations through rigid body transformations using geometric primitives such as points, lines, and surfaces, as summarized in Table 3. Typically, a minimum of three pairs of these corresponding geometric elements is required to establish a robust transformation model. These methods vary significantly in their algorithmic robustness, computational complexity, and sensitivity to structural saliency. Among these approaches, point-based registration is commonly applied for global registration, which relies on accurate extraction and matching of shared features across adjacent stations. Early feature extraction algorithms, such as point feature histograms (Rusu et al., 2009), spin images (Johnson et al., 1999), and scale-invariant feature transforms (Barnea et al., 2007), often exhibited high sensitivity to noise, limited robustness, high computational cost, and reduced registration accuracy in complex environments (Kang et al., 2009; Wang et al., 2008). To mitigate these issues, Hänsch et al. (2014) and Gressin et al. (2013) proposed a series of area-based registration methods that utilize the geometric and topological properties of feature regions. These approaches significantly improved the robustness and accuracy of feature point extraction, especially under complex tunnel scenarios. Further enhancements were achieved through the development of the 4-point congruent sets (4PCS) (Aiger et al., 2008) and its

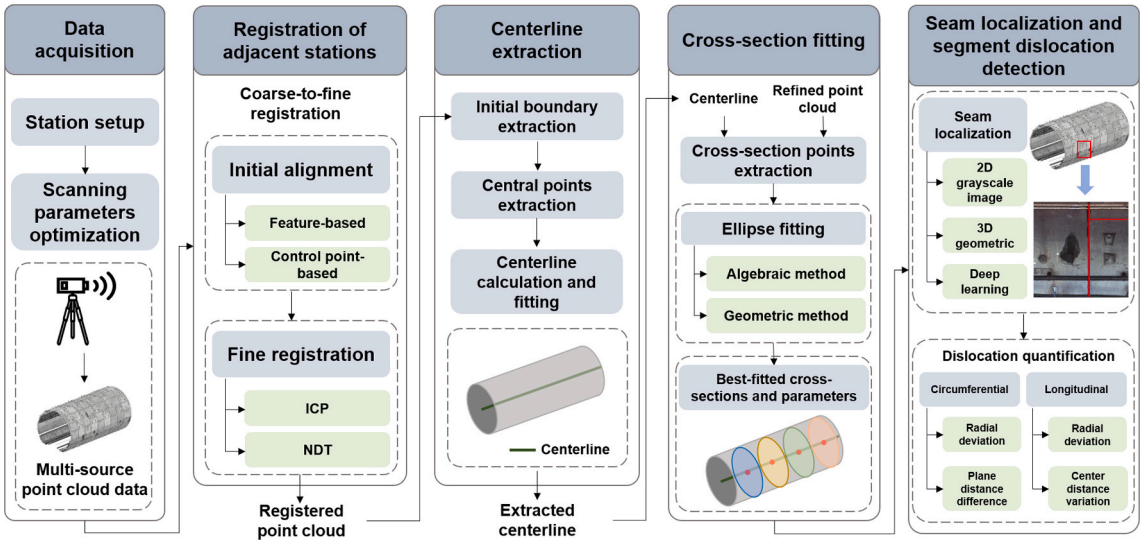


Fig. 8. General technical framework for shield tunnel deformation monitoring using laser scanning point clouds.

Table 3
A summary of geometric-based registration methods, including their specific techniques, key improvements, and limitations.

Geometric feature	Source	System	Specific method	Improvements	Limitations
Point-based	Barnea and Filin (2007)	TLS with Co-mounted Camera	Computation of Rigid body transformation	– Image-assisted geometric refinement; – Minimal 3-point RANSAC estimation; – Automatic, targetless operation.	– Accuracy sensitive to camera–scanner calibration; – Reduced performance with increased scan baseline.
	Gressin et al. (2013)	ALS and TLS	Improved ICP algorithm	– Robustness under complex tunnel scenarios.	– Limited performance.
	Sun et al. (2020c)	Vehicle-mounted LiDAR system (MLS)	4-point congruent sets (4PCS)	– Improved efficiency; – Enhanced robustness.	– Reduced matching stability in feature-sparse scenes.
Line-based	Yang et al. (2015)	ALS and TLS	Laplacian matrix decomposition	– Overcoming density and view differences between ALS and TLS.	– Highly dependent on the presence of buildings.
Surface-based	Dold and Brenner (2004)	TLS	Least Squares 3D Surface Matching (LS3D)	– High flexibility; – Sensitivity of sub-noise.	– Sub-optimal accuracy on small or flat targets.
	Monserrat and Crosetto (2008)	TLS	Automatic Registration via Planar Patches	– Target-free operation; – Automatic process.	– Limited accuracy; – Manual correspondence matching.

extended version, super 4PCS, proposed by Sun et al. (2020c). By employing coplanar four-point bases, these methods demonstrated increased tolerance to noise and outliers, improving overall registration accuracy. Nevertheless, such methods require sufficient overlap between adjacent scans and the presence of distinct geometric features such as tunnel joints, seams, or structural edges to achieve reliable matching (Cheng et al., 2018).

In contrast to point-based approaches, line-based registration methods, such as line feature translation (Von Hansen et al., 2008), Laplacian matrix decomposition (Yang et al., 2015), and segmentation using triangulated irregular networks (TIN) (Lee et al., 2007), utilize the geometric continuity and topological constraints inherent in linear structures to facilitate point cloud alignment. Owing to their higher-order abstraction, linear primitives offer more potent geometric constraints than discrete points, typically yielding superior registration precision and numerical stability (Al-Durgham et al., 2014; Habib et al., 2005). Such attributes render them exceptionally effective for large-scale 3D mapping scenarios, such as long tunnel sections and underground corridors (Cheng et al., 2018). Nonetheless, their effectiveness is strictly contingent upon the robust extraction of linear features, which remains challenging under high-noise or within irregular structural morphologies.

Surface-based registration methods exploit the holistic geometric characteristics of planar or curved manifolds, making them less sensitive to noise and capable of achieving higher registration accuracy. Techniques including least squares fitting (Monserrat et al., 2008), conjugate surface feature methods (Dold et al., 2004), and principal component analysis (PCA) capture global structural regularities from tunnel linings, sidewalls, and structural facades to provide stable, comprehensive alignment frameworks. While line-based and surface-based methods demonstrate high theoretical precision, their effectiveness relies on the availability of geometrically feature-rich structures with well-defined morphological signatures. In featureless environments, maintaining reliable registration accuracy remains a persistent challenge (Brenner et al., 2008).

In summary, the evolution of point-, line-, and surface-based methods highlights a general trajectory toward enhanced algorithmic robustness and reduced sensitivity to the stochastic noise and geometric repetitive symmetries characteristic of tunnel environments.

(2) Control point-based registration methods

Control point-based registration methods utilize predefined reference points within the tunnel environment as spatial anchors to align point clouds acquired from different scanning stations. These control points, often established through precise geodetic surveying, serve as fixed positional benchmarks that enable all point clouds to be consistently transformed into a unified global coordinate system. This approach is particularly advantageous in environments characterized by sparse geometric features or repetitive structural elements, such as tunnels, where traditional feature-based extraction methods may struggle to provide reliable registration. By utilizing pre-established control points, the method minimizes registration errors and ensures consistent alignment between point clouds from adjacent scanning stations. However, this type of method is constrained by the labor-intensive and time-consuming deployment and measurement of control points, especially in long or complex tunnel environments. Accurate placement, visibility assurance, and repeated surveying of control points require meticulous planning and execution. Despite these logistical challenges, the method remains a preferred strategy for high-precision applications, such as long-term tunnel deformation monitoring, safety assessment, and structural diagnostics in shield tunneling projects.

(3) Iterative closest point (ICP) and normal distributions transform (NDT)

In contrast to feature- and control point-based methods, ICP and NDT achieve alignment by directly optimizing the spatial proximity within overlapping regions, without requiring explicit feature extraction or external reference points. This makes them more flexible and easier to implement in practical tunnel monitoring scenarios.

The ICP algorithm remains a foundational paradigm for fine point cloud registration (Wang et al., 2012). It operates by iteratively minimizing the sum of squared Euclidean distances between identified point correspondences within the overlapping regions of adjacent scans, thereby estimating the optimal rigid body transformation. Despite the simplicity and widespread application, its performance remains highly contingent upon a precise initial pose and is susceptible to stochastic noise and outliers. As an alternative, NDT-based registration employs a probabilistic representation of the underlying geometry. It discretizes the point cloud into a three-dimensional voxel grid, where each cell is characterized by a Gaussian probability density function (PDF) reflecting the spatial distribution of points. By maximizing the likelihood of point-to-distribution matches, NDT offers increased robustness to sensor noise and exhibits a smoother convergence landscape.

In shield tunnel scenarios, the characteristic high-overlap between adjacent scans significantly benefits ICP and NDT-based solvers. In such environments, these direct methods often surpass conventional feature-based techniques, which are frequently compromised by the repetitive structural symmetries and low geometric saliency of tunnel linings (Yang et al., 2021). However, to achieve optimal performance and mitigate error propagation, these methods typically require rigorous preprocessing, including point cloud down-sampling, denoising, or outlier removal.

The registration methods discussed above exhibit distinct advantages and limitations, and their suitability depends on tunnel geometry, surface characteristics, and specific monitoring goals. Geometric feature-based methods are particularly effective in environments with abundant and well-defined structural features, whereas control point-based approaches provide enhanced reliability in geometrically uniform or feature-sparse scenarios. Registration methods such as ICP and NDT provide a practical balance between accuracy and computational efficiency, making them well-suited for routine tunnel monitoring tasks. Future progress is expected from hybrid registration strategies that integrate the advantages of existing methods. AI-based automated feature extraction will provide an additional pathway for improving the accuracy and efficiency of tunnel point cloud registration.

4.2. Optimization of scanning parameters and TLS locations

In TLS-based tunnel deformation monitoring, the quality and reliability of the point cloud largely depend on its ability to accurately capture the tunnel surface geometry. Several stochastic and systematic variables govern range measurement precision, most notably the incident angle, scanning distance, atmospheric conditions, and the reflective properties of the tunnel lining.

While the hardware specifications and material properties are often predetermined, operational parameters remain adjustable to optimize data fidelity. Central to these is the incidence angle. As this angle increases approaching a grazing incidence, the backscattered signal intensity attenuates significantly, thereby escalating range uncertainty and coordinate error. This degradation is more pronounced in shield tunnels with circular or elliptical cross-sections, where the curved tunnel surface makes it difficult to maintain a near-orthogonal incidence angle. Similarly, extended scanning range results in reduced point density and increased susceptibility to noise, driven by beam divergence and atmospheric interference. Such constraints are critical for high spatial resolution diagnostics, where insufficient point density may obscure subtle structural anomalies, such as cracks or minor spalling, leading to potential misinterpretation of structural health.

Early evaluations of TLS performance established the fundamental geometric relationship between acquisition setup and point precision. Van Gosliga et al., 2006 and Soudarissanane et al. (2009) quantified the sensitivity of ranging precision to incidence angle and scanning ranges. Their findings underscore a deterministic inverse correlation between acquisition range/angle and coordinate accuracy, as shown in Fig. 9. Van Gosliga et al., 2006 further proposed a pragmatic 20-meter range threshold to minimize data degradation in circular tunnels. Subsequent studies by Lindenbergh et al. (2005) and Lam (2006) also highlighted the importance of scanner placement, surface segment selection, and point density control to enable precise deformation monitoring using the Leica HDS3000 system. Moreover, Fekete et al. (2010), Gikas (2012), and Roca-Pardiñas et al. (2014) further investigated tunnel geometry inspections from a practical standpoint. However, no comprehensive methodology for point cloud optimization was proposed. Building on this foundation, Pejić (2013) proposed a framework that incorporates incident angle and point-density distribution into an integrated model for determining optimal scanner positioning along the tunnel alignment. This scheme offered a systematic solution to improve point cloud quality and enhance the precision for deformation monitoring. More recently, Cabo et al. (2017) proposed an algorithmic paradigm for automated scan planning. Their methodology dynamically determines a minimum set of scanner positions and their optimal locations while satisfying predefined quality constraint, such as minimum overlap and incidence angle limits, as illustrated in Fig. 10. This transition from heuristic station setting to algorithmic optimization marks a significant advancement in the operational efficiency and precision under practical application scenarios.

Optimizing scanning parameters and TLS locations is critical for enhancing point cloud quality and ensuring reliable deformation monitoring in tunnel environments. Key strategies include: (1) minimizing incident angles to improve the precision of range measurements, (2) maintaining scanning distances within recommended limits, e.g., typically not exceeding 20 m to reduce data degradation caused by beam divergence and atmospheric effects, and (3) ensuring sufficient point density to capture fine-scale structural features critical for deformation assessments.

Future research should emphasize the integration of advanced optimization algorithms, including machine learning (ML), to automate scanner positioning and parameter configuration. These advancements will further streamline tunnel monitoring workflows and enhance the precision of TLS-based deformation analysis.

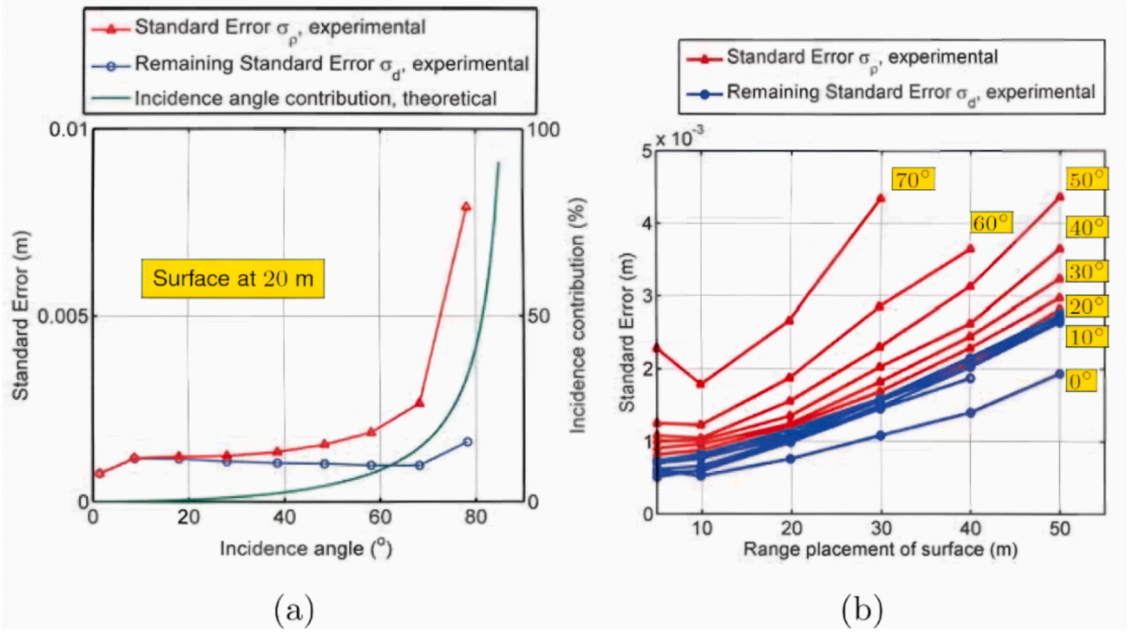


Fig. 9. Measurement precision with respect to (a) the incident angle of the surface and (b) the range placement of the surface. In both figures, the remaining standard error is obtained after removal of the incident angle effect (Soudarissanane et al., 2009).

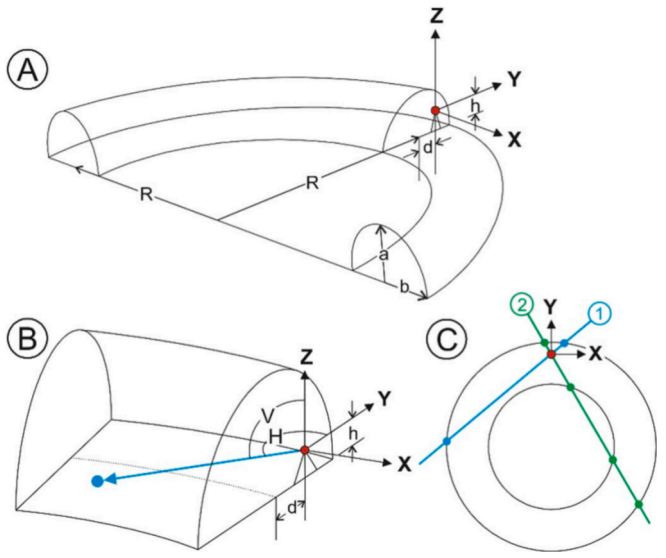


Fig. 10. Toroidal tunnel parameters defining the shape of the tunnel (Cabo et al., 2017).

4.3. Centerline extraction

The accurate extraction of the tunnel centerline is a crucial step in shield tunnel deformation detection. Defined as a curve fitted through the centers of successive tunnel cross-sections, the centerline serves as a geometrically meaningful reference for evaluating tunnel integrity. As the axis of structural symmetry, it provides a basis for quantifying geometric deviations from the design profile and for monitoring long-term deformation. Accurate centerline extraction is therefore essential for structural health assessment, geometric analysis, and the development of maintenance and repair strategies.

In recent years, numerous point cloud-based methods have been developed for centerline extraction, each tailored to specific tunnel conditions and acquisition systems. Fig. 11 demonstrates the general workflow of centerline extraction. Typically, the central points of the cross-section on the XOY or YOZ plane are first extracted through a range of methods. These methods can be classified into two main categories: (a) geometric feature–based approaches that rely on surface normal information; and (b) point cloud projection-based methods on different coordinate planes. Based on the previously obtained central points, the tunnel centerline can be calculated through iterative central curve fitting and center calculation. Regardless of the specific approach, their effectiveness is closely related to the quality of the acquired point cloud, which in turn is influenced by the choice of scanning technology. In shield tunnels, three primary data acquisition systems are commonly used: TLS, Section-based MLS, and Panoramic MLS.

(1) TLS

TLS employs a station-based scanning approach characterized by high precision and stable point cloud acquisition. However, achieving comprehensive scene coverage requires multiple scanning stations due to constraints such as station positioning and scanning geometry. Numerous methods have been developed to extract tunnel centerlines from TLS-registered point clouds, most of which exploit the geometric characteristics of tunnel structures.

Point cloud projection methods have emerged as a widely used technique for extracting tunnel due to their algorithmic simplicity and

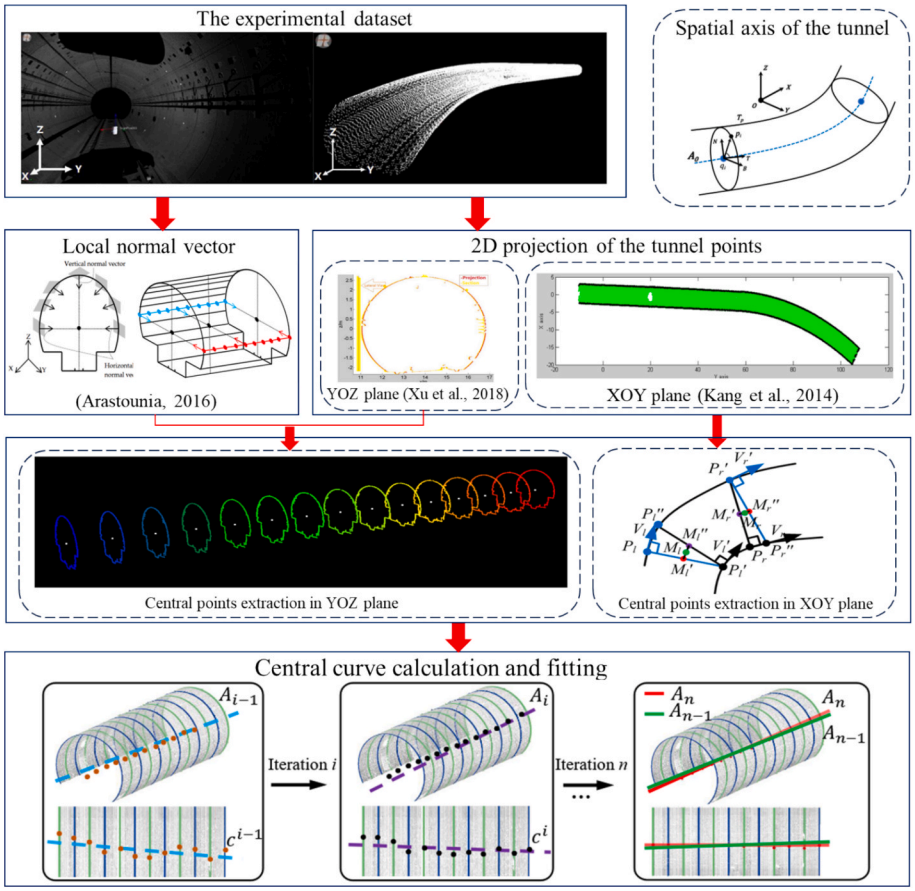


Fig. 11. The general workflow for the centerline extraction (Arastounia, 2016; Kang et al., 2014; Xu et al., 2018b; Yi et al., 2020).

low computational cost. Early studies primarily utilized 2D projection strategies. By projecting 3D tunnel coordinates onto optimized planar domains, structural boundary features can be delineated, followed by robust geometric fitting using algorithms such as Random Sample Consensus (RANSAC) (Kang et al., 2014; Xu et al., 2018b). These approaches achieve millimeter-level accuracy but exhibit high sensitivity to scanning noise and are contingent upon the fidelity of the initial boundary segmentation. To enhance robustness and accommodate diverse tunnel geometries, subsequent research transitioned toward cross-sectional slicing and geometric model-based fitting strategies. For instance, Xie et al. (2017) proposed a global cylindrical fitting approach for 3D tunnel reconstruction, which enhances computational efficiency and provides more stable stochastic estimates of the centerline. However, since shield tunnels typically comprise a complex sequence of straight sections, curves, and transition curves, a rigid cylindrical fitting method is primarily suited for straight tunnels and may struggle to accurately handle curved segments. To address these geometric complexities, Yi et al. (2020) proposed a hybrid framework integrating iterative circular cross-sectional fitting with B-spline interpolation to model complex curved alignments. Cao et al. (2019) further refined this process through a density-based slicing methodology. By employing an enhanced RANSAC algorithm coupled with a Minimum Spanning Tree (MST) approach, their method effectively partitions the tunnel into linear and circular primitives while optimizing the spatial continuity of the extracted centerline. Additionally, Savitzky-Golay smoothing (Savitzky et al., 1964) is implemented as a post-processing step to mitigate high-frequency noise and ensure the derivative continuity of the final alignment.

(2) Section-based MLS

Compared with static TLS, MLS provides greater flexibility and mobility, making it particularly suitable for long and continuous tunnel environments. Among MLS techniques, section-based MLS has demonstrated significant advantages in recent years for deformation monitoring and structural assessment in shield tunnels.

Tunnel centerlines extracted from section-based MLS data typically utilize one of the following strategies: (a) Direct extraction from MLS trajectory data. It relies on vehicle trajectory data captured by the MLS system. Puente et al. (2016) utilized inertial navigation data to compute the centerline directly from the MLS path, assuming accurate georeferencing of the start and end points. (b) Geometric fitting-based methods that use tunnel geometry. Arastounia (2016) fitted local planes to the tunnel surface and used the direction of normal vectors to isolate side walls. Midpoints of line segments connecting opposite wall points are used to define centerline points, which are then connected to form the full centerline. (c) Rotation projection density variance (RPDV). To address the roughness and uncertainty of tunnel surface point cloud data, Zhang et al. (2019) introduced the RPDV-based centerline extraction algorithm. It identifies the optimal rotation angle that minimizes the variance in projected point cloud density, thus enabling robust centerline extraction even in irregular or noisy tunnel data, without requiring knowledge of the scanner's position relative to the tunnel axis.

(3) Panoramic MLS

The application of panoramic mobile laser scanning (PMLS) has grown rapidly in extensive corridor environments requiring seamless and continuous data coverage, such as urban roads, highways, and railways. These systems are also referred to as Mobile Mapping System (MMS) or Mobile Laser Scanning and Imagery (MLSI) platforms (Choo et al., 2024; Kim et al., 2022), typically integrate panoramic cameras with directional laser scanners to achieve comprehensive environmental mapping through multi-sensor fusion techniques (Li et al., 2024; Reulke et al., 2004). Recent literature highlights two distinct developmental trajectories: the pursuit of cost-effective accessibility versus high-end precision. For instance, Jian et al. (2025) developed a lightweight, self-designed MMS for subway tunnels that utilizes a spinning mid-range LiDAR (SML) within a robust multi-sensor fusion framework to provide a viable alternative to expensive commercial platforms. Conversely, high-performance architectures integrated with 360-degree laser scanners, such as the RIEGL VMX-2HA (Beloch et al., 2024), have set new benchmarks in data fidelity. These systems directly acquire full-surround point cloud data without requiring image fusion, which is particularly beneficial in tunnels with complex and variable geometries. The high-density and uniformly distributed point cloud data captured by PMLS supports a range of advanced applications: (1) detailed 3D modeling, the dense and uniform data enables the reconstruction of highly accurate 3D representations of tunnel infrastructure; (2) structural analysis and deformation monitoring, the geometric fidelity and spatial continuity improve the precision of structural assessment and safety diagnostics. Furthermore, the compatibility of PMLS data with established analytical techniques, such as tunnel central axis extraction and cross-sectional profiling, enhances its versatility for infrastructure monitoring and condition evaluation tasks.

4.4. Cross-section fitting

A tunnel cross-section refers to the two-dimensional profile of a tunnel at a specific location, oriented perpendicularly to the centerline. Accurate extraction and fitting of these cross-sections are essential for analyzing tunnel structural stability, assessing deformation patterns, and supporting engineering decision-making.

A variety of methodologies have been developed to extract tunnel cross-sections, ranging from semi-manual operations to fully autonomous point cloud processing pipelines. Early studies primarily utilized projection-based and central-line-driven strategies. Han et al. (2013b) proposed a method that extracts the tunnel centerline via morphological skeletonization of a 2D projection map. They further aligned the y-axis with the tunnel centerline to extract transverse slices, employing a spatial buffer to isolate the relevant point subsets for subsequent deformation analysis (Han et al., 2013a). While effective, these methods relied heavily on interpolation from a reference point cloud, meaning the deformation analysis accuracy was directly affected by the raw point cloud density. Subsequent research introduced more refined geometric fitting and boundary extraction techniques. Kang et al. (2014) identified boundary points in a 2D plane using a moving window and fitted them via the RANSAC algorithm, followed by cross-section fitting using a quadric parametric surface. Similarly, Cheng et al. (2016) delineated boundary points through an angular search criterion on a 2D projection manifold. The cross-sections were subsequently refined based on locally estimated centerlines and upper boundary lines. By identifying boundary points using criteria such as distance, angle, or moving window strategies, these methods enhanced the numerical stability of cross-section estimation. However, many of these approaches assumed tunnel alignment in the horizontal plane and required additional optimization to improve fitting accuracy.

A major limitation of many conventional methods lies in their idealized geometric assumptions, which often fail to account for the non-uniform deformations induced by complex structural interactions. Therefore, ellipse-fitting techniques are widely used to characterize tunnel cross-sectional geometry for structural analysis and deformation assessment, as shield tunnels are typically approximated as circular or elliptical in shape. These techniques can be broadly categorized into the algebraic ellipse fitting methods and the geometric ellipse fitting methods, as illustrated in Fig. 12.

(1) Algebraic ellipse fitting methods

Algebraic methods derive ellipse parameters by solving the general conic equation using linear or nonlinear least-squares regression. These methods aim to minimize algebraic distances and estimate parameters

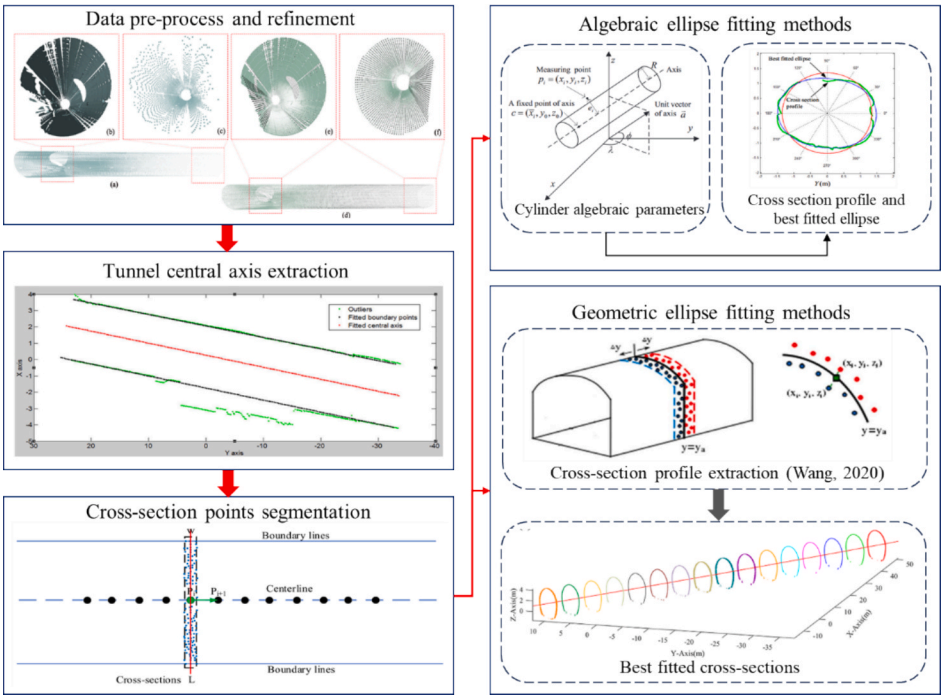


Fig. 12. Graphical illustration for ellipse fitting methods (Cao et al., 2019; Wang et al., 2020; Xie and Lu, 2017; Yu et al., 2022).

such as the lengths of the major and minor axes, the centroid location, and the rotation of the axes. Xie et al. (2017) developed a non-iterative algorithm using matrix computations to estimate ellipse parameters and construct a 3D tunnel model for convergence analysis. Additionally, Yu et al. (2022) developed a robust spatial circle fitting method that used a previously extracted horizontal centerline to define cross-section planes. Points within a defined proximity threshold were projected onto these planes and the circle center and radius were then estimated to satisfy both plane and spherical geometric constraints, enabling efficient sequential extraction. These approaches are computationally effective and provide direct analytical solutions for the elliptic parameters such as axis lengths, center position, and orientation of the fitted ellipse. However, the minimization of algebraic distance rather than geometric error may introduce biased estimates, particularly under high-noise conditions or when the point distribution is non-uniform.

(2) Geometric ellipse fitting methods

In contrast to algebraic methods, geometric methods focus on minimizing the Euclidean distance between point cloud points and their corresponding points on the fitted ellipse, emphasizing features such as the center of the ellipse, the major and minor axis lengths, and inclination angles of the axes. For example, Wang et al. (2020) introduced a rotary-inertia-based approach to determine ellipse orientation. By computing the principal and secondary axes of inertia, the method directly estimates axis lengths and orientation, thereby defining the optimal ellipse. Furthermore, Sun et al. (2022) highlighted the limitations of prior studies in handling irregular geometries. They identified the intersection points between the cross-sectional planes and lines connecting point pairs from either side of tunnel surface. A cubic B-spline curve was then fitted to these points to construct a smooth and accurate cross-section profile. These methods exhibit superior resilience to stochastic noise and are more adept at capturing complex, non-idealized structural morphologies.

4.5. Seam localization and segment dislocation detection

Accurate detection of segment dislocations in shield tunnels is essential for ensuring structural integrity, supporting long-term maintenance, and preventing potential failures. Dislocations typically occur at segment seams, which are classified into two types: circumferential seams between rings and longitudinal seams between segments within a ring. Precise seam localization thus serves as the foundation for reliable dislocation analysis and overall tunnel health monitoring. Currently, two primary technologies are employed for seam localization and dislocation detection: total station measurement and MLS. As the most widely used measuring instrument in tunneling operations, the total station improves efficiency compared to traditional methods. However, due to constraints in measuring angles, the requirement for continuous repositioning imposes operational complexity and time consumption, making it difficult to meet the efficiency demands of large-scale shield tunnel inspections. In contrast, MLS has emerged as a dominant and advanced solution for detecting segment dislocations (Liu et al., 2023a). Its non-contact operation, high spatial resolution, and rapid data acquisition capabilities make it highly suitable for the tunnel environment. MLS can efficiently capture large-scale three-dimensional point cloud data of tunnel linings, enabling robust detection of seams and accurate quantification of displacements. With the increasing scale and complexity of shield tunnels, the transition from traditional total station methods to MLS-based workflows represents a critical step toward intelligent, data-driven tunnel maintenance.

To achieve accurate seam localization, various grayscale image-based, point cloud-based geometric, and deep learning (DL)-based methods have been proposed for this purpose (Sun et al., 2020b; Xu et al., 2022), as illustrated in Table 4.

(1) Grayscale image-based methods

In these approaches, 3D tunnel point cloud data are projected onto 2D planes to generate grayscale intensity images, where seams typically appear as low-intensity regions relative to surrounding areas (Yue et al., 2021). For instance, Du et al. (2019) analyzed grayscale images to calculate intensity gradients and effectively identified the left and right edges of circumferential seams by detecting gradient peaks, as illustrated in Fig. 13. Additionally, the inherent linearity of seams has further facilitated the application of image processing techniques. Du et al.

Table 4
Methods of Segment Seam Localization for Shield Tunnel 3D Point Clouds.

Method type	Source	System	Specific method	Performance	Accuracy
Gray image-base methods	Du et al. (2019)	TLS and MLS	Integrating peak detection	– Equipment-free operation; – Continuous positioning.	deviation = 2.3 cm RMSE = 0.02 m
	Sun et al. (2020b)	MLS	Grayscale gradient calculation	– High-resolution imaging; – Efficient positioning.	Deviation <3 mm RMSE <5 mm
	Yue et al. (2021)	MLS	Canny edge detection and Hough transform	– High efficiency; – Multi-source data.	Longitudinal deviation <2 mm Angle deviation <3°deviation <1 mm
	Xu et al. (2022)	Self-Driven MLS	Canny edge detection and Hough transform	– Fully automatic operation; – Rapid data acquisition.	transverse seam error $<1.85 \times 10^{-2}$ mm deviation <3 mm
	Du et al. (2022)	MLS and TLS	Gradient accumulation method	– High automatic extraction rate and efficiency.	accuracy = 2.3 cm deviation <1 mm; extraction rate 100%
Point cloud-based geometric methods	Shen et al. (2025)	TLS	Hough transform; MSAC; 3σ criterion	– High recognition rate; – Robustness for hard-to-detect longitudinal seams.	Recognition rate: 100% for circumferential seams; 88.4% for longitudinal seams
	You and Wang (2025)	MLS	Ellipse fitting residuals and deep feature clustering	– Adaption to non-uniform deformation.	Dislocation detection error ≤ 0.002 m
DL methods	Yu et al. (2021)	MLS	Dual deep CNN framework	– High automatic extraction rate and efficiency; – Robustness against occlusion.	Average location error = 1.567 pixels Deviation = 2 mm
	Ji et al. (2022a)	MLS	Encoder-Decoder Based Segment Seam Localization	– High processing efficiency; – Anti-interference.	detection rate = 100% IoU = 89.2% RMSE = 1.8 mm
	Li et al. (2023)	MLS	GL-Net DL network	– High processing efficiency; – Robustness against occlusion; – Multi-scanner compatibility.	IoU = 51.76% – 59.12% detection rate = 98.88% – 100%

(2022) employed Hough Transform to detect longitudinal seams on grayscale images. Furthermore, Xu et al. (2022) and Sun et al. (2020b) combined the Canny edge detection and Hough Transform with grayscale statistical information to accurately localize circumferential seams and longitudinal seams. However, these traditional methods are sensitive to image quality degradation caused by tunnel aging, surface wear, and environmental noise, which can compromise localization accuracy.

(2) Point cloud-based geometric methods

Geometric methods operate directly on 3D point clouds without projecting to 2D planes, thereby avoiding information loss and format conversion errors (Shen et al., 2025). These methods typically exploit the distinct morphological signatures of seams, such as localized planarity offset and radial discontinuities, in combination with tunnel design parameters for seam localization and segment segmentation. Different strategies are adopted for circumferential and longitudinal seams. For instance, Shen et al. (2025) integrated the Hough transform within a cylindrical coordinate system with M-estimator Sample Consensus (MSAC) to resolve circumferential joint planes with high

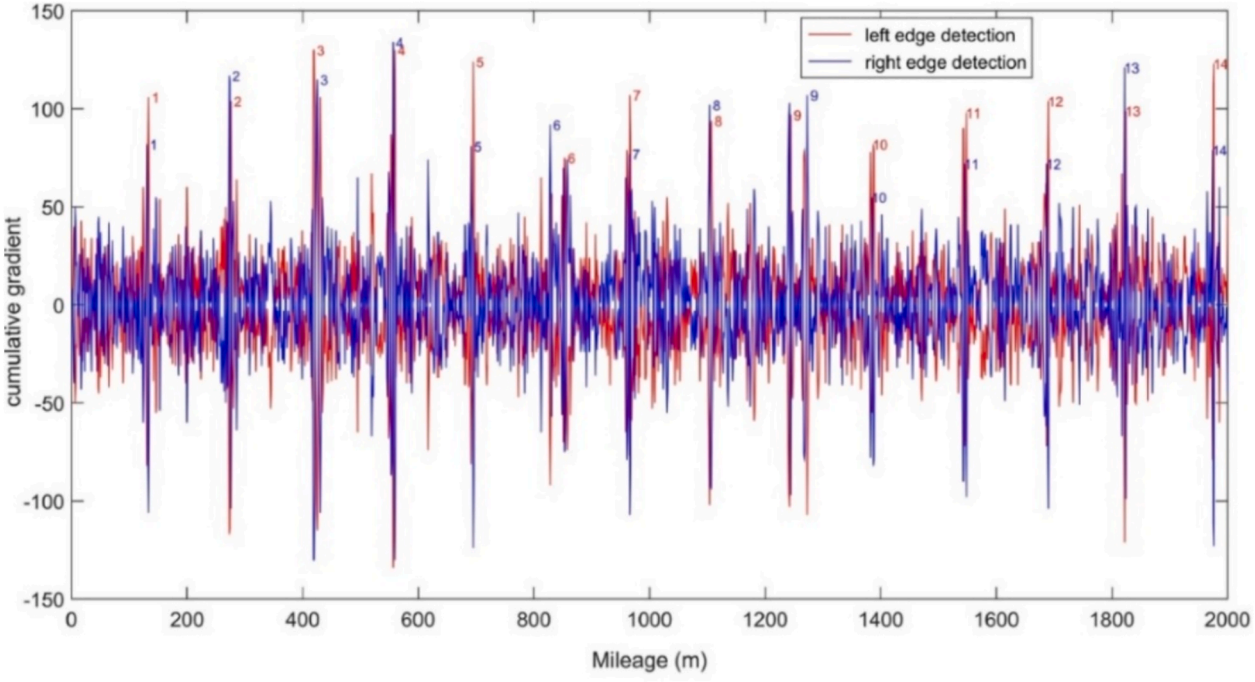


Fig. 13. Intensity gradient-based peak detection method (Du et al., 2019).

precision. For longitudinal seams, statistical 3σ criterion was applied to identify endpoint coordinates based on tunnel design priors. Meanwhile, You et al. (2025) addressed the challenge of segment dislocation detection under non-uniform deformation by utilizing ellipse fitting residuals for noise filtering and deep feature clustering for seam localization. Through piecewise elliptical fitting of individual segments, this framework achieves precise dislocation quantification with errors within 0.002 m, significantly outperforming traditional circle-fitting methods in complex structural environments. While these unsupervised methods offer superior computational efficiency without requiring extensive labeling, their reliability remains contingent upon the density of the point cloud and the precision of the underlying structural priors.

(3) Deep learning-based methods

To overcome the limitations of classical image processing, DL models have been introduced to improve seam detection accuracy under complex conditions. Yu et al. (2021) proposed a dual-CNN model designed to detect circumferential and longitudinal seams in depth images, demonstrating superior performance compared to conventional techniques such as Canny, Sobel, and Hough operators. However, the performance of deep-learning approaches can degrade when tunnel-lining deterioration produces low-contrast or heavily noise-affected images. To mitigate these challenges, the geometric correlation between bolt holes and seams is leveraged in existing approaches. Ji et al. (2022b) utilized an improved Cloth Simulation Filter (CSF) algorithm to extract bolt holes from grayscale images and employed the Density-Based Spatial Clustering of Applications with Noise (DBSCAN) algorithm to remove noise. Seam positions were then inferred using a Mean Shift algorithm and the designed spatial layout of bolt holes, enabling the localization of both circumferential and longitudinal seams, as shown in Fig. 14. Similarly, Cui et al. (2019) adopted a template matching strategy based on bolt hole locations to identify longitudinal seams. However, the effectiveness of these methods largely depends on the accuracy of bolt hole extraction. In specific shield tunnel installations, bolt holes are sealed with cement to prevent leakage, thereby obscuring their geometry and significantly reducing extraction accuracy. Recent advances in artificial intelligence have led to the development of point cloud-based DL models that enable direct three-dimensional seam segmentation. Li et al. (2023) introduced the GL-Net model, which effectively segments multiple tunnel elements, including circumferential seams, longitudinal seams, bolt holes, clutter, cables, and grouting holes, from raw point clouds. Additionally, Ji et al. (2022a) proposed an encoder-decoder-based DL model that effectively segments seepage regions, including circumferential seams, longitudinal seams, and bolt holes. These methods offer significant improvements in localization precision and generalizability across varying tunnel conditions. Lin et al. (2025b) developed LiningNet, a geometry-informed network incorporating bi-neighborhood feature aggregation and geometric label encoding to capture the specific unique structural signatures of segmental linings. This domain-specific approach significantly outperforms general-purpose large-scale point cloud segmentation architectures like SparseUNet (Choy et al., 2019) and SCF-Net (Fan et al., 2021). However, their broader applicability is hindered by several challenges. One major limitation lies in the requirement for large volumes of training data. Additionally, the significant sample imbalance among different tunnel elements introduces biases into the model, limiting its generalizability and effectiveness.

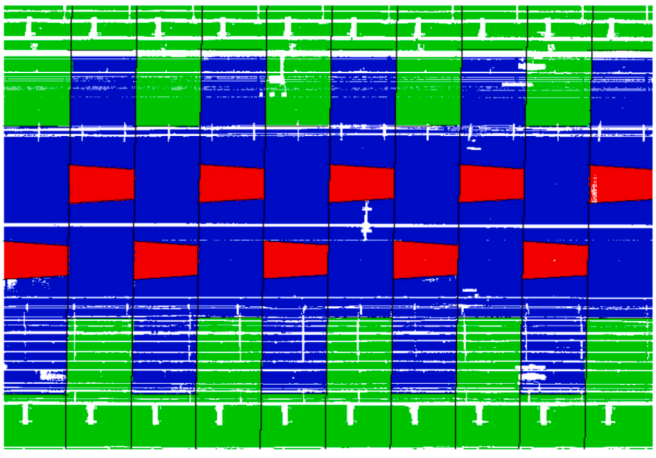


Fig. 14. Circumferential and longitudinal seams detection results (Ji et al., 2022b).

After seam localization, circumferential dislocations are commonly evaluated by fitting the cross-sectional point clouds on both sides of the circumferential joints and quantifying the misalignment. For instance, Du et al. (2022) fitted the point clouds into two circular arcs and computed the radial deviation between the arcs to measure the dislocation, as illustrated in Fig. 15. This geometric deviation provides a direct indication of the relative offset between adjoining segments. Additionally, Cui et al. (2024a) utilized DL networks to segment tunnel elements and identify areas of interest (AOIs) corresponding to circumferential joints. Each AOI was fitted to a plane, and the elevation differences between the adjacent planes were calculated to quantify vertical dislocation. Similarly, Yu et al. (2021) extracted localized point cloud subsets adjacent to circumferential joints and applied the RANSAC algorithm to fit each subset to a plane. The dislocation was then computed as the distance between the two fitted planes, offering a robust estimate that accommodates data irregularities. Longitudinal dislocations are typically analyzed based on the geometric configuration of blocks within an individual ring, as illustrated in Fig. 16. For instance, Du et al. (2022) fitted the entire ring into an elliptical model and calculated the average distance from the points of each block to the center of the ellipse. The dislocation between adjacent blocks was then quantified by calculating the difference in these average distances, which reflects block-wise radial displacement. Similarly, Cui et al. (2019) adopted a polar coordinate system to represent point cloud data on either side of longitudinal seams. By comparing the radial coordinate differences, the relative displacement between blocks was effectively estimated. In terms of 3D data-driven approach, Lin et al. (2025a) introduced an automated high-fidelity reconstruction of segmental tunnel lining geometry to quantify structural deformation. These methods collectively establish a robust framework for the detection and quantification of both circumferential and longitudinal dislocations, which is essential for monitoring shield tunnel performance and identifying potential structural risks. However, despite their effectiveness, these methods are susceptible to point cloud noise, particularly during the fitting of circular arcs, planes, or ellipses. Noise and outliers can significantly affect the precision of the fitted geometric models, thereby compromising the accuracy of dislocation measurements.

4.6. Comparative analysis of TLS and MLS

TLS and MLS are two key technologies employed for deformation monitoring in shield tunnels. Both systems are capable of capturing precise three-dimensional geometric data. However, they differ significantly in terms of data acquisition workflows, point cloud characteristics, and operational complexity, which directly influence their effectiveness in various tunnel monitoring scenarios.

As illustrated in Fig. 17, TLS and MLS follow distinct operational pipelines. TLS typically involves a multi-step process including adjacent station point cloud registration, scanning parameter optimization, and scanner position optimization. These steps reflect the metrological complexity of static acquisition, which prioritizes high local point density and ranging precision. In contrast, MLS collects point clouds with relatively uniform density due to its dynamic, continuous scanning mechanism. Furthermore, the disparate point density distributions of

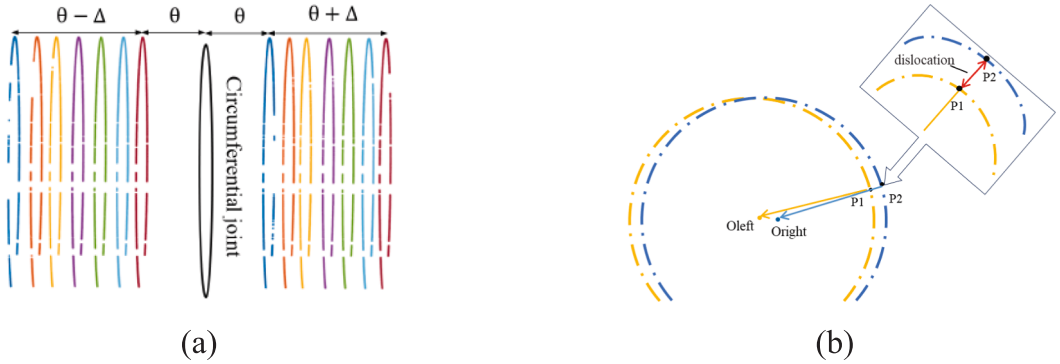


Fig. 15. The schematic of circumferential dislocation detection (Du et al., 2022). (a) Cross-section selection for detecting circumferential dislocation. (b) Circumferential dislocation calculation.

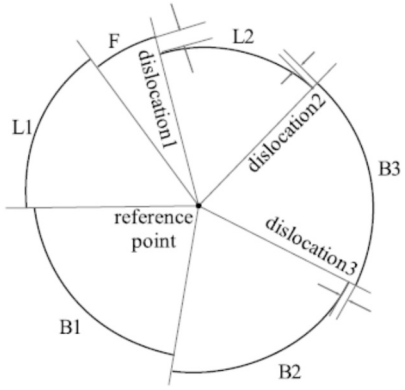


Fig. 16. The schematic for longitudinal dislocation (Du et al., 2022).

these two modalities significantly influence the robustness of centerline extraction algorithms. TLS inherently produces a radially decaying density profile relative to the fixed scan center, a consequence of its static perspective, whereas MLS provides more continuous coverage along the tunnel axis. However, MLS may provide lower point density in localized areas than TLS, which can limit the detection of fine-scale structural defects. Despite these variations, the two systems follow the same steps in cross-section fitting, seam localization, and segment dislocation detection, as depicted in Fig. 17. This consistency underscores their reliability in conducting essential geometric analyses for deformation monitoring.

In summary, while TLS and MLS demonstrate distinct characteristics in preliminary data acquisition and density distribution, their analytical capabilities converge in key deformation monitoring tasks. TLS offers high-resolution, high-accuracy data ideal for detailed inspection and long-term deformation analysis, whereas MLS provides rapid, large-scale scanning capabilities suited for operational efficiency and real-time monitoring. Leveraging the strengths of both technologies through integrated deployment strategies can enhance both the efficiency and accuracy of deformation assessments in shield tunnels, offering a more comprehensive approach to structural health monitoring.

5. Defect detection in shield tunnels using laser scanning point cloud data

5.1. Common defects and characteristics in shield tunnels

Shield tunnels are subject to complex structural and environmental conditions that significantly influence their structural integrity. They are

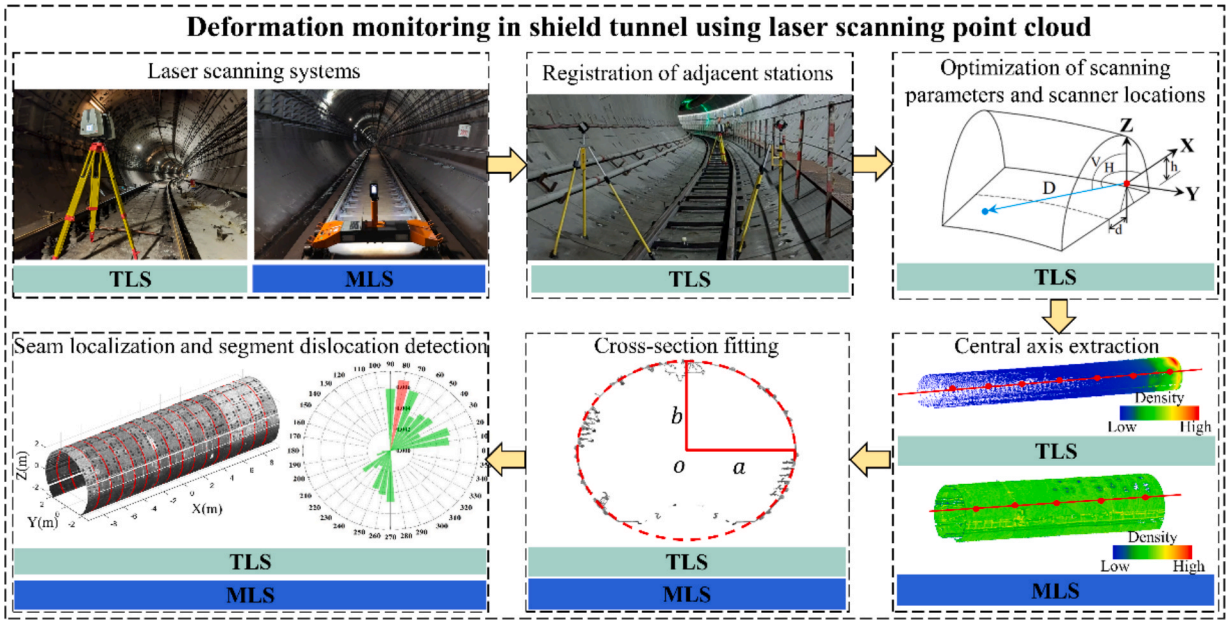


Fig. 17. The difference between TLS and MLS for deformation monitoring.

typically constructed using prefabricated concrete segments, which are assembled to form continuous ring structures (Yi et al., 2019). While this modular construction allows for flexibility and ease of installation, it also introduces numerous joints and interfaces that act as potential weak zones susceptible to defects over time. Due to their subterranean location, shield tunnels are subjected to a range of external forces, including overburden pressure from surrounding strata, lateral soil movement, and hydrostatic pressure from groundwater (Lin et al., 2022; Xie et al., 2021). Additionally, geological heterogeneity and fluctuating groundwater levels induce stress redistribution and non-uniform deformation across the tunnel lining, further exacerbating structural vulnerabilities.

As a result of these complex loading conditions and long-term environmental exposure, shield tunnels commonly exhibit three types of structural defects: water leakage, cracking, and lining spalling. Leakage often occurs at segment joints, where gaps or compromised seals enable groundwater ingress. Prolonged exposure to moisture deteriorates concrete matrix and promotes secondary defects. Cracks arise from cyclic train loads, differential settlement, or thermal shrinkage. These fractures compromise structural continuity and create pathways for water ingress, which in turn accelerates degradation. Spalling results from the progressive disintegration of concrete, often initiated by persistent water exposure or reinforcement corrosion, leading to detachment of surface layers and exposure of deeper structural elements. These phenomena are effectively visualized and assessed using laser scanning point cloud data, as illustrated in Fig. 18.

This non-contact measurement technique enables high-resolution documentation of surface morphology and material reflectivity, providing a robust basis for defect detection. Leakage areas typically exhibit lower intensity values in the point cloud data due to laser signal absorption and scattering by water (Sanchiz-Viel et al., 2021), as shown in Fig. 18(a). This intensity-based feature offers a reliable cue for distinguishing moist areas from intact concrete surfaces. Cracks appear as linear discontinuities or voids in the point cloud data, characterized by sharp, narrow gaps or depressions, as shown in Fig. 18(b). Their detectability depends on width and depth relative to the scanning resolution. Lining spalling, which involves surface material detachment, manifests as localized concave deformations with irregular textures. These rough and uneven surfaces indicate further degradation of the tunnel lining, as shown in Fig. 18(c). Understanding the geometric and reflectance signatures of these defect types facilitates the development of automated detection and classification algorithms based on point cloud data. By leveraging the high spatial resolution and radiometric fidelity of terrestrial or mobile laser scanning systems, the accuracy and efficiency of tunnel defect assessment can be substantially improved, supporting proactive maintenance and safety evaluation.

5.2. Leakage detection

Leakage in shield tunnels refers to the infiltration of groundwater through structural discontinuities such as segment joints or bolt holes, posing significant risks to structural integrity and accelerating tunnel degradation (Attard et al., 2018; Wang et al., 2022c). Traditionally, leakage detection has relied heavily on manual visual inspection, wherein trained personnel identify visible signs of moisture or seepage on tunnel surfaces. Although this approach provides direct confirmation, it is inherently labor-intensive, time-consuming, and subject to human error and subjectivity. With the advancement of photogrammetric technologies, mobile inspection systems equipped with linear CCD cameras have been developed to acquire high-resolution images of tunnel linings (Huang et al., 2018; Huang et al., 2017; Li et al., 2021). These image datasets are subsequently analyzed using image processing techniques to detect leakage patterns (Feng et al., 2023; Huang et al., 2017; Xue et al., 2018), as illustrated in Table 5. However, image-based approaches are highly sensitive to lighting conditions, which are often inadequate in tunnel environments. Moreover, surface texture variations can mimic leakage features, leading to false positives and reduced detection reliability.

LS technology has emerged as a promising alternative due to its ability to operate in poor lighting conditions and provide intensity information. Therefore, intensity-based thresholding can be applied, where low-intensity regions are flagged as potential leakage zones (Lu et al., 2019; Xu et al., 2018a). However, intensity thresholds are not universally applicable, as they vary across different tunnel environments and scanning configurations, thus limiting the generalizability and robustness of such methods.

To address these limitations, some studies convert 3D point clouds into 2D intensity images by projecting the tunnel vault onto a planar surface (Guo et al., 2024; Huang et al., 2020; Yin et al., 2023). This transformation enables the application of mature image-based techniques, such as Otsu thresholding (Wang et al., 2022b) and region extraction strategies such as connected component analysis (Sun et al., 2020b), for identifying leakage areas. While these methods offer improved computational efficiency, they remain susceptible to environmental variability and external noise affecting intensity values. To improve robustness and leakage detection accuracy, recent efforts have increasingly turned to DL models. Among them, Fully Convolutional Networks (FCNs) have been widely applied to tunnel inspection tasks, demonstrating notable performance over conventional image processing methods (Feng et al., 2023; Xue et al., 2018). In particular, Mask R-CNN has attracted significant attention due to its strong instance segmentation capability, achieving robust performance across diverse tunnel environments (Chen et al., 2024b; Huang et al., 2020; Xue et al., 2022). For instance, Cheng et al. (2021) developed an enhanced FCN based on the VGG-19 model, specifically designed to segment leakage regions in intensity images. Additionally, Liu et al. (2022a) incorporated a residual network module, namely Res2Net, within a cascade framework to extract multiscale features from leakage regions, significantly improving detection performance. These DL-based frameworks and modules significantly augment leakage detection efficacy by extracting high-level, discriminative semantic features to precisely delineate leakage areas within intensity images.

However, despite these developments, challenges remain in accurately identifying leakage in shield tunnels. Leakage frequently emerges at structural discontinuities such as segment joints, bolt holes, and grouting holes, where precast concrete segments are connected (Yin et al., 2023; Yu et al., 2018), as depicted in Fig. 19. These areas are more susceptible to groundwater infiltration, leading to leakage patterns with distinct geometric and structural characteristics. Methods relying solely on intensity images may not fully capture the three-dimensional spatial context of these features, limiting their effectiveness in complex environments. To overcome these limitations, researchers have explored methods that directly utilize three-dimensional point cloud data. Unlike intensity-based approaches, point cloud-based methods preserve spatial and geometric information, enabling more accurate leakage identification (Wang et al., 2022c; Wang et al., 2024b). Notably, Li et al. (2023)

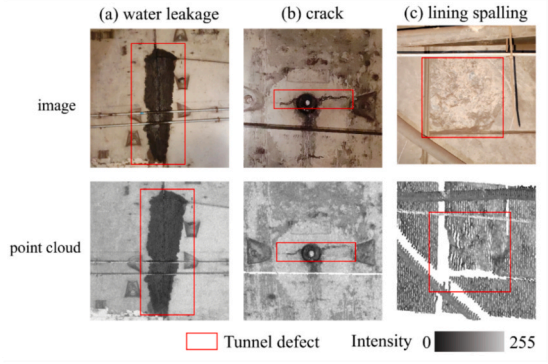


Fig. 18. Image and point cloud data of different tunnel defects.

Table 5
A summary of water leakage detection methods, including their performance, key improvements, and limitations.

Method type	Source	System	Specific Method	Performance	Advantages	Limitations
Image-Based Inspection	Huang et al. (2017)	Line-scan CCD camera	Otsu threshold segmentation and crack recognition algorithm	Recognition accuracy >87% Detection speed: 3–5 km/h; assembly/disassembly time 5 min/3 min	– High data acquisition efficiency; – Intuitive presentation.	– Greatly affected by illumination; – Poor robustness; – Lack of 3D position of leakage.
	Huang et al. (2018)	Line-scan CMOS cameras	FCN-based two-stream semantic segmentation algorithm	Average error rate = 0.8%	– Robustness in overlapping areas; – High semantic segmentation accuracy.	– High computational requirements; – High miss rate for small-area leakage; – Relies on manual annotation.
	Xue and Li (2018)	Line-scan CCD cameras	R-FCN-based two-stage detection	Classification accuracy = 95.84% Detection rate = 94.40%	– High localization accuracy; – High detection speed.	– Large amount of annotated data required; – High computational cost.
	Li et al. (2021)	Line-scan cameras	Improved Faster RCNN	MAP = 88.50% Recall = 97.00% Precision = 93.60% Detection speed: Maximum 15 km/h	– Simultaneous detection of multiple defects; – Lightweight equipment.	– High computational cost; – Poor robustness; –Massive annotated data required.
	Feng et al. (2023)	Open-source water leakage dataset	UNet/UNet++ combined with 6 types of encoders	UNet-EfficientNetB6: IoU = 84.97% UNet++-EfficientNetB5: IoU = 87.70% Error rate <5.00%	– Balanced accuracy and efficiency; – Pixel-level segmentation; – Quantification of water leakage area.	– High computational complexity; – Limited segmentation accuracy; – Dataset diversity required.
Laser Scanning-Based Methods	Huang et al. (2020)	MLS	Mask R-CNN for instance segmentation	Segmentation accuracy: MPA = 97.18% MioU = 77.05%	– Detailed output information; – Capable of distinguishing adjacent small leakages.	– Large computation load; – Curvature error in 2D point cloud projection; – High equipment cost.
	Yin et al. (2023)	MLS and line-scan camera	improved YOLOv5	Defect detection accuracy: Average F1 = 84.20% surface defect F1 = 71.40%	– Robust capable of detection; – Precise 3D spatial information.	– Time-consuming preprocessing; – Insufficient generalization ability.
	Guo et al. (2024)	MLS and line-scan camera	RDES-Net	F1 increased by 2.20%; mAP increased by 5.20%.	– Strong anti-interference ability; – Excellent real-time performance.	– Prone to missing small-area water leakage; – High annotation cost; – Poor robustness.

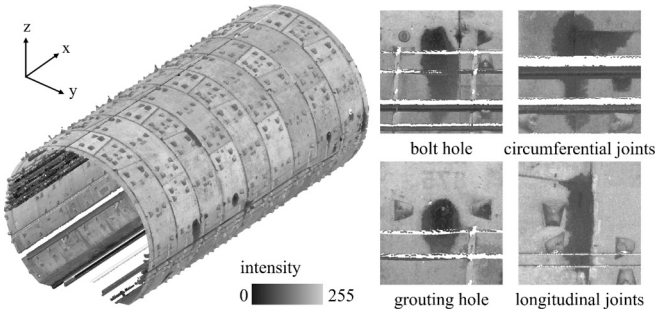


Fig. 19. The spatial characteristics of the location of tunnel leakage.

proposed a point-based semantic segmentation approach that enhances accuracy by directly analyzing raw point cloud data. Their method integrates global and local feature learning, improving the detection of structural anomalies. Similarly, Ji et al. (2022a) developed an encoder-decoder DL model for multi-class segmentation, including leakage detection. Their approach normalizes point clouds and constructs voxel-based inputs for the encoder-decoder network, allowing the model to effectively learn spatial features.

Despite the advantages of 3D point cloud-based methods, several challenges persist. One major issue is computational complexity. Processing large-scale point cloud datasets requires substantial computational resources, often necessitating high-performance computing environments or specialized hardware. This requirement limits the accessibility of such methods, particularly for organizations with limited computing infrastructure. Another challenge is the enormous data volume. The high density and precision of point cloud data generate massive datasets, requiring significant storage and processing capabilities. Real-time or near-real-time leakage detection remains difficult due to the time-intensive nature of data processing. Additionally, leakage instances are relatively rare compared to normal tunnel surfaces, leading to class imbalance in datasets. This imbalance can cause bias in detection models, reducing their sensitivity to leakage areas. Addressing this issue requires optimized algorithms, improved data augmentation strategies, and advanced learning techniques to enhance model robustness. Future research should focus on improving the efficiency of 3D point cloud processing, developing adaptive learning models, and leveraging emerging computing technologies to enhance real-time detection capabilities. By addressing these challenges, point cloud-based leakage detection can become a reliable and scalable solution for tunnel maintenance and safety assessment.

5.3. Crack and defect detection

Cracks in tunnel structures are defined as fractures or separations within the tunnel lining, typically induced by mechanical stress, material fatigue, or environmental factors. These discontinuities can compromise the structural integrity of the tunnel over time, posing risks to operational safety and longevity. Traditionally, crack detection has relied heavily on manual visual inspections, where inspectors assess tunnel surfaces to identify and measure crack width, length, and distribution. Simple tools such as crack gauges or rulers are sometimes employed to improve measurement accuracy. While manual inspection

allows real-time observation, it is inherently subjective, depending on the expertise of the inspector, and prone to inconsistencies. Moreover, it is time-consuming and labor-intensive, limiting its practicality for large-scale inspections, especially in environments such as tunnels where access may be difficult. Manual approaches also struggle to detect micro-cracks or accurately quantify crack depth, thereby limiting their value in comprehensive structural assessments. To address these limitations, photogrammetry-based methods have been developed utilizing high-resolution images to detect and quantify surface-level cracks (Zhang et al., 2014). These image-based methods enable non-contact detection and have shown potential in various applications (Liao et al., 2022; Liu et al., 2022b; Zhang et al., 2021). However, they remain highly sensitive to environmental factors such as lighting conditions, shadows, and surface textures. Additionally, while photogrammetry provides excellent surface detail, it often lacks depth information, limiting its ability to characterize the three-dimensional morphology of cracks.

In recent years, laser scanning technologies, particularly TLS and MLS, have emerged as a powerful tool for crack detection in tunnels (Murakami et al., 2018). These technologies produce high-density point cloud data, offering both geometric and intensity information of the tunnel surface (Zhou et al., 2023).

(1) TLS offers extremely dense and accurate point clouds, as shown in Fig. 20(b). Its high spatial resolution enables the detection of small and narrow cracks, which may be invisible in lower-resolution datasets. However, TLS requires frequent repositioning of the scanner, resulting in increased inspection time and labor costs. This localized scanning strategy limits TLS efficiency when applied to long tunnel sections.
(2) MLS, in contrast, enables continuous, high-speed scanning along the tunnel path, greatly enhancing data acquisition efficiency. However, due to its lower point density, MLS may fail to detect fine or micro-cracks, particularly those with widths below a few millimeters, as shown in Fig. 20(c). Despite this, MLS remains suitable for detecting more prominent cracks and offers a practical balance between coverage and resolution.

Laser scanning facilitates crack detection by capturing reflectivity variations and surface geometry. Cracks typically exhibit different laser reflection properties compared to intact surfaces, making them distinguishable using intensity variations. The geometric and intensity information also supports the precise detection and quantitative assessment of crack attributes such as width and depth, which are critical for evaluating structural defects. One effective technique involves intensity gradient analysis, wherein cracks are identified based on sharp intensity transitions. Algorithms such as Canny edge detection are commonly employed to delineate crack boundaries. For instance, Yang et al. (2020) demonstrated that applying dilation operations and edge detection to TLS data significantly reduces false detections and enhances delineation accuracy. Similarly, Xu and Yang (2019) further refined this approach using Gaussian filtering, which effectively suppresses noise while preserving crack edge details. Despite these advancements, laser scanning technologies remain insufficient in some contexts. LS lacks the fine visual detail necessary to distinguish small surface cracks, particularly in low-contrast scenarios, whereas cameras lack depth and geometric information, which is essential for assessing crack morphology and tunnel deformation. To address these complementary limitation, Jeong et al. (2023) developed a hybrid approach combining 3D LS with a Pan-Tilt-Zoom (PTZ) camera system, which integrates high-resolution images with laser scanning data. This approach enables real-time tracking of crack propagation with improved precision. To address the limitation of insufficient intensity features, Jing et al. (2025) proposed a novel 3D multimodal feature named 3DMulti-FPFHI that lies in the fusion of geometric information encoded by FPFH and a 3D intensity feature. This 3DMulti-FPFHI directly fuses features in 3D space, helping mitigate intensity inconsistencies caused by environmental variations and enabling simultaneous detection of geometric and non-geometric anomalies without extensive training.

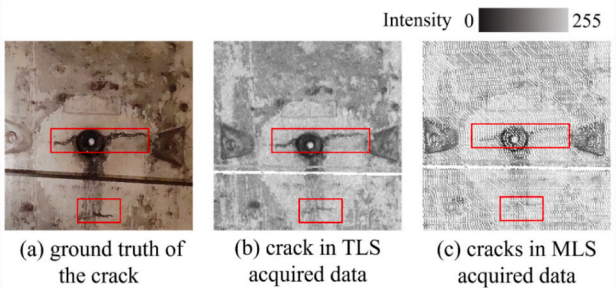


Fig. 20. The manifestation of cracks in TLS and MLS acquired point cloud data.

Beyond initial detection, point cloud data enables detailed geometric analysis of crack features. Crack width can be estimated by measuring the lateral distance between opposing point clusters along the crack margins, while depth can be inferred from the vertical displacement of points within the crack relative to adjacent surfaces. These metrics are critical for assessing the severity of the crack and guiding appropriate maintenance decisions.

Despite the advantages of laser scanning for crack detection, several challenges remain. One of the primary difficulties is noise within the point cloud data, particularly in areas with high reflectivity or where the tunnel surface has complex geometries. Noise can cause false positives, where small surface irregularities are mistaken for cracks. To mitigate this issue, advanced filtering techniques, such as Gaussian filtering, are frequently employed to reduce noise and retain significant features. Another challenge is occluded areas, particularly at segment joints or tunnel corners, where portions of the surface are blocked from the sight of the scanner line. In such cases, multi-station scanning is often necessary to achieve full coverage, further increasing inspection time and complexity.

In summary, while TLS and MLS have proven effective for crack detection and measurement in shield tunnels, ongoing challenges such as data noise, occlusions, and micro-crack resolution highlight the need for integrated multi-sensor approaches, optimized algorithms, and efficient data processing pipelines, as summarized in Table 6. Continued development in these areas is essential for achieving scalable, automated, and high-precision tunnel health monitoring systems.

5.4. Spalling detection

Lining spalling in shield tunnels refers to the detachment of concrete fragments or protective surface layers from the tunnel lining, resulting in localized surface degradation and exposing the internal material to environmental stressors (Yin et al., 2023). This form of defect not only weakens the mechanical integrity of the tunnel lining but also increases vulnerability to water ingress, which may accelerate reinforcement corrosion, leading to further deterioration and potential safety risks. Traditionally, spalling has been identified through manual visual inspections, where inspectors look for exposed aggregates, flaking surfaces, or hollow sounds upon tapping with hammers or probes. While such methods allow for direct human judgment, they are time-consuming, subjective, and inconsistent. Manual inspection is often unable to detect incipient spalling or subsurface delamination, leading to underestimation of defect severity. The effectiveness of these traditional methods is further constrained by operator experience and limited surface coverage during routine inspections.

With the advent of advanced sensing technologies, LS provides a modern and effective solution for detecting tunnel lining spalling. By generating high-resolution 3D point cloud data, LS accurately captures the surface geometry of tunnel linings, allowing for precise detection of small surface irregularities that might be overlooked during a manual

Table 6
A summary of various crack detection methods.

Source	System	Method	Performance	Advantages	Limitations
Xu and Yang (2019)	TLS	Gaussian filtering	Best parameter: $\sigma = 2.1$ SNR = 0.47 gradient = 0.1	– High efficiency and full automation.	– Dependent on parameter selection; – Sensitive to noise.
Yang and Xu (2020)	TLS	Dilation and Canny edge detection	Detection error = 2.92%	– No requirement of parameter determination; – Applicable to both vertical and horizontal cracks.	– Inapplicable to tilt cracks.
Liu et al. (2022b)	Line-scan COMS camera	Improved pixel-level image processing and structural analysis	Recognition rate: 100% for simple images, 91.15% for complex images Optimal inspection speed 18 km/h	– Strong anti-interference; – Good illumination adaptability; – High practicality for lightweight system; – Better performance in complex scenes.	– Easily to miss weak-feature cracks; – Pixel-only width output; – Limited detection range; – Manual threshold adjustment required.
Liao et al. (2022)	Area-scan CCD cameras	LinkCrack detection network	F1-score = 88.25% Precision = 91.56% Recall = 85.17%	– High-speed detection capability; – Lightweight deployment and high efficiency; – Suitable for long crack recognition; – Strong data compatibility.	– Limited detection range; – Relatively low accuracy; – Light sensitivity.
Jeong et al. (2023)	3D LS and PTZ camera system	MSML Mask DCNN	mAP at KEPRI, HIT-B107, and SS sites are 83.60%, 80.30%, and 41.40% respectively	– High robustness in complex scenarios.	– Dependence on manual markers; – High computational cost; – Insufficient narrow crack detection.
Jing et al. (2025)	TLS	PatchCore	Maintaining robustness but relatively low F1-score	– No extensive training; – Low data requirement; – Avoids 2D projection information loss.	– Struggles with narrow cracks (<0.02 mm); – Massive noise introduced along with intensity information.

inspection. Compared to traditional methods, LS offers several key advantages: (1) objective and repeatable measurements, reducing subjectivity and human error, (2) potential for automated data processing and scalable analysis, enhancing inspection efficiency and comprehensiveness, and (3) high-resolution data acquisition, enabling early detection of minor surface irregularities. One of the primary geometric features used for detecting spalling is surface roughness. Spalled regions typically exhibit increased irregularity and textural variation, distinguishing them from intact concrete surfaces (Wu et al., 2019). Surface roughness can be quantitatively assessed by converting point cloud data into triangular mesh grids, which represent local surface morphology, as illustrated in Fig. 21. A common metric for roughness is the surface-to-projected area ratio, where a higher ratio indicates more pronounced surface deviations. Wu et al. (2019) employed this approach and proposed a roughness descriptor for detecting concrete spalling using 3D MLS data, which effectively distinguishes spalling regions from typical structural elements such as bolt holes, grouting ports, and segment seams. Despite the effectiveness of roughness-based techniques, they have inherent limitations. Many structural features such as bolts and seams can mimic the geometric signature of spalling, resulting in false positives. Furthermore, roughness alone cannot capture underlying material loss or assess the depth of degradation. To address these issues, researchers have turned to DL techniques for automated spalling detection. These methods can learn complex spatial and intensity features from laser scanning data, significantly improving detection accuracy. For example, Zhou et al. (2021) proposed a deep convolutional neural network (DCNN)-based framework named the Spalling Intensity Depurator Network (SIDNet), which leverages MLS-acquired intensity images, depth maps, and spatial features to identify spalling defects. This approach integrates geometric and reflectance cues to improve detection accuracy by reducing false positives caused by bolt holes and seams, automatically quantifying of defect severity using depth and intensity variation, and reconstructing spalling regions to enhance visualization and digital monitoring. By integrating intensity-based

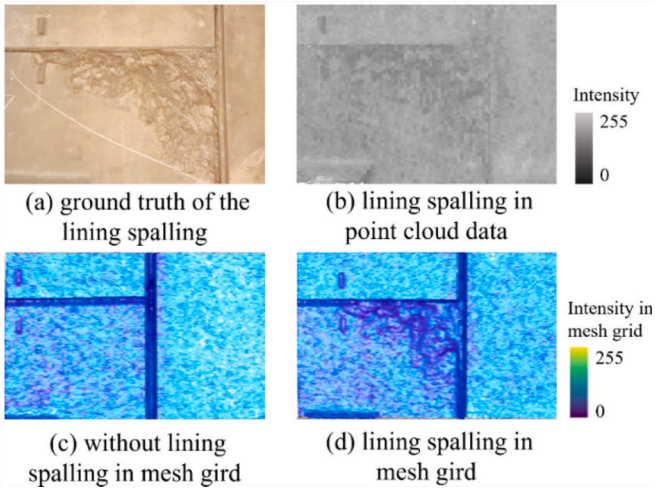


Fig. 21. The manifestation of lining spalling in point cloud data and mesh grid.

analysis with DL-driven segmentation, SIDNet demonstrated significant improvements in efficiency and precision compared to traditional manual or geometric roughness-based approaches.

Despite the promise of laser scanning and DL for spalling detection, several challenges remain. One major issue is the presence of noise, which can result from factors such as the scanning resolution, sensor movement, and environmental conditions such as moisture and dust. Noise not only affects surface roughness estimation but also complicates the extraction of fine features. Another persistent challenge is the semantic ambiguity between spalling and other common tunnel surface artifacts. Sophisticated models are required to achieve accurate classification across varying tunnel environments and construction types. Moreover, DL-based approaches are computationally intensive and

require large, annotated datasets for training. In practice, the availability of labeled tunnel spalling data is limited, and domain adaptation remains an open problem. Additionally, real-time or near-real-time processing remains difficult due to the high computational cost of 3D data handling. Optimization strategies such as model compression, adaptive resolution processing, and hybrid inference architectures are needed to bridge this gap.

5.5. Defect classification and severity assessment

The heterogeneous characteristics of tunnel defects captured in point cloud data present significant challenges for developing generalizable and robust detection algorithms. Defect types, including cracks, leakage, and lining spalling, exhibit highly diverse spatial distributions, geometries, and reflectivity patterns. This heterogeneity complicates the application of conventional rule-based or handcrafted feature extraction methods, which typically lack the flexibility to adapt across varying defect types, shapes, scales, and textural properties. DL techniques, particularly those based on convolutional neural networks (CNNs), provide a promising alternative by automatically learning hierarchical representations of defect features in a data-driven manner (Kuang et al., 2022). These models can exploit both spatial geometry and intensity variations within point cloud data to identify and classify multiple defect types simultaneously. Recent advances in image-based tunnel inspection systems have demonstrated the efficacy of deep neural networks in multi-defect detection (Li et al., 2021; Wang et al., 2022a; Xu et al., 2021; Zhang et al., 2024a), providing a strong foundation for extending such approaches to 3D point cloud data.

However, the application of DL for multi-defect detection using point cloud data remains limited due to several practical constraints, including: (1) The complexity of annotating point cloud data: Unlike 2D images, labeling 3D point clouds requires specialized tools and significantly more effort due to higher dimensionality and the limited availability of mature annotation frameworks; (2) The computational demands of processing large-scale 3D data: DL models require extensive computing resources to efficiently learn spatial relationships and fine-grained defect characteristics in point clouds. Developing comprehensive, annotated datasets and optimizing neural network architectures for 3D multi-defect classification remains a key area of research in tunnel infrastructure monitoring. Overcoming these limitations requires the development of efficient 3D data labeling tools, standardized benchmark datasets, and lightweight yet expressive neural network architectures tailored for real-time or near-real-time tunnel inspection applications.

Beyond defect detection, defect severity assessment is crucial for maintenance prioritization and risk management. Different defect types require distinct metrics for severity evaluation, which can be effectively extracted from point cloud data. Leakage severity is typically assessed by the extent of the affected surface area. In point clouds, leakage is often indicated by reduced intensity values due to water absorption, which attenuates laser reflectivity. Projecting low-intensity regions onto a 2D unwrapped tunnel lining surface enables accurate quantification of leakage spread (Gao et al., 2019), providing early warning of potential waterproofing failures. Crack severity is primarily characterized by width and depth, which can be derived by analyzing the spatial coordinates of points along the crack profile: (1) crack width is estimated by calculating the lateral spacing between points on opposing crack edges; (2) crack depth is inferred from the vertical offset between points within the crack and the adjacent undamaged surface (Zhou et al., 2023). Accurate dimensional analysis of cracks allows for the distinction between superficial surface fissures and structurally significant fractures, thereby guiding appropriate remedial strategies. Lining spalling severity is typically evaluated using: (1) the spalled surface area, quantified by identifying regions of high surface roughness in the point cloud; (2) the material loss depth, obtained by measuring the deviation of the spalled region from the expected tunnel lining profile (Wu et al., 2019). By constructing a 3D mesh, these deviations from the normal tunnel lining can be detected, allowing for precise calculations of spalling depth and area. This enhances the accuracy of defect quantification, supporting more effective repair planning and resource allocation. Point cloud data provides both geometric and intensity information, enabling a comprehensive evaluation of defect severity. Geometric features, such as 3D depth, width, and surface roughness metrics enables volumetric and structural quantification, whereas intensity-based features can capture surface condition changes. By combining these complementary modalities, tunnel operators can achieve more accurate, objective, and data-driven severity assessments, ultimately improving the efficiency, reliability, and safety of tunnel infrastructure maintenance.

5.6. Deep learning-based defect detection

In recent years, the exceptional capability of DL methods in capturing complex spatial patterns has significantly accelerated their application in downstream tunnel inspection tasks, such as leakage (Liu et al., 2025; Zheng et al., 2024) and lining spalling detection (Zhou et al., 2021). However, for certain defects such as cracks, which commonly occur at centimeter or even millimeter scales in shield tunnels, the direct application of DL techniques to point cloud encounters substantial limitations. The primary constraint lies in the limited resolution and inherent sparsity of point cloud data, which impede the reliable detection of such discontinuities. To address these limitations, multi-modal data fusion has emerged as a promising approach for crack detection. By integrating point cloud data with complementary modalities such as high-resolution optical imagery or thermal infrared imaging, this fusion strategy leverages the geometric precision of 3D point clouds alongside the fine texture and thermal contrast captured in images (Huang et al., 2014). The resulting multi-modal representations can improve the detection and characterization of small surface cracks.

To systematically summarize the recent progress in this field, Table 7 provides a comprehensive performance comparison of representative deep learning models. DL-based tunnel defect detection methods can be broadly classified into two main paradigms. One widely adopted strategy involves converting 3D point cloud data into 2D intensity images, subsequently applying conventional 2D DL architectures. This strategy allows the use of established models, including mask-based methods (Chen et al., 2024b; Huang et al., 2020; Qian et al., 2025), YOLO-based methods (Yin et al., 2023), and attention-based (Guo et al., 2024; Zhang et al., 2022) methods, for defect identification. The backbone networks associated with these methods consistently demonstrate strong capabilities in capturing spatial features, effectively handling object detection and segmentation tasks, and exhibiting robust performance against varying environmental conditions. Building upon these standard architectures, numerous enhancements have been proposed, including refined feature extraction techniques (Chen et al., 2024b; Guo et al., 2024), multi-scale feature fusion modules (Liu et al., 2022a; Zhang et al., 2023), and expanded receptive fields (Zhang et al., 2022), which further boost their detection performance. Despite notable advancements, these methods inherently possess critical limitations. Many tunnel defects are inherently irregular 3D structures, such as lining spalling manifesting as recessed areas and leakage typically localized around bolt holes and segment joints (Jiang et al., 2025). Such characteristics underscore the need to preserve spatial relationships and geometric details between points. However, the process of transforming 3D point clouds into 2D representations inherently leads to the loss of critical spatial and geometrical information. The resulting methods rely primarily on intensity values and planar topological structures, thereby diminishing detection accuracy. Additionally, the subsequent necessity to reproject detection results back into three-dimensional space introduces further complexities, reducing the practicality and effectiveness of such non-end-to-end methods for engineering applications.

In contrast, another category of approaches directly processes raw 3D point cloud data, inherently preserving the geometric fidelity and

Table 7
Performance comparison of state-of-the-art deep learning-based models for tunnel surface and structural defect identification.

Paradigm	Reference	Backbone Network	Modification	Target Defect	Performance
3D point cloud to 2D projection	Zhang et al. (2022)	U-Net	– Dual attention network; – Pixel-wise weighted cross-entropy loss.	Seepage	IOU = 66.00% Precision = 73.60% Recall = 86.40% F1 = 79.50%
	Yin et al. (2023)	YOLOv5	– Coordinate attention; – BiFPN; – GhostConv.	Dislocation, Water leakage, Spalling.	mAP = 90.30% Recall = 78.90% F1 = 84.20%
	Chen et al. (2024b)	Mask R-CNN	– Cylindrical-voxel structure.	Water leakage	mAP = 92.02% mIoU = 87.49%
Raw 3D point cloud	Ji et al. (2022a)	Custom Encoder–Decoder	– Voxelization and 3D Convolution.	Seepage	F1 = 83.29% IoU = 71.37%
	Li et al. (2023)	Custom GL-Net	– Global and local feature encoding block; – Weighted cross entropy loss function.	Longitudinal and circumferential joints, bolt holes, grouting holes, cables, clutter.	mIoU = 73.02%
	Jiang et al. (2025)	Point Transformer	– Geometry enhanced channel attention block.	Water leakage	mIoU = 92.38% mAcc = 94.50%

spatial context. These methods typically focus on adaptively learning intricate spatial relationships among points exploiting modules such as 3D convolutional neural networks (3D CNNs) (Ji et al., 2022a), global and local feature encoding (Li et al., 2023), and positional embeddings (Jiang et al., 2025). The explicit consideration of spatial distributions and geometric structures significantly enhances the accuracy and robustness of defect identification. These direct 3D methods have demonstrated commendable performance and generalization capabilities across diverse tunnel environments. Nevertheless, their computational complexity remains an essential limitation. The computational resource associated with directly processing large-scale, sparse, unordered, and irregular point cloud data is notably high. This potentially restricts their applicability in real-time inspections as efficiency during short operational windows is paramount. Additionally, the unstructured nature of point cloud data necessitates increasingly sophisticated neural network architectures, posing challenges for efficient implementation. Despite these challenges, DL techniques directly utilizing 3D point cloud data offer substantial potential for advancing tunnel defect detection.

6. Challenges in LS data processing and potential solutions

6.1. Large-scale data processing

Laser scanning systems generate high-density point clouds essential for accurately capturing the geometric and structural details of tunnel environments. However, these datasets can reach terabyte- to petabyte-scale, posing significant challenges in terms of storage, efficient processing, and management.

(1) Data storage and management

Storing large-scale LS datasets requires robust and scalable systems that can handle continuous data without sacrificing accessibility. Traditional storage solutions often struggle with scalability, read/write speeds, and metadata management, which are critical for efficient indexing and retrieval. To address these issues, distributed storage systems, such as the Hadoop Distributed File System (HDFS), provide scalable storage capable of handling massive LS datasets across multiple nodes (Ahmed et al., 2023). Advanced data compression algorithms, such as Octree (Qin et al., 2024) and Voxel Grid (Lyu et al., 2024), effectively reduce data volume while preserving critical geometric detail, enhancing storage efficiency. Metadata tagging can further enhance retrieval speed, aiding rapid access for subsequent processing.

(2) Computational challenges in processing large datasets

Processing high-resolution point clouds typically involves computationally intensive tasks such as denoising, feature extraction, registration, and deformation analysis. As dataset size increases, the computational load grows substantially, frequently surpassing the limits of traditional single-node processing environments. To enhance computational efficiency, several strategies have been proposed: (1) parallel and distributed computing: frameworks such as Apache Spark (Paredes et al., 2024) and Google Cloud Dataflow (Akidau et al., 2021) partition large datasets into smaller subsets, enabling simultaneous processing across distributed computing nodes and significantly reducing total computation time and enhancing scalability; (2) GPU acceleration: Utilizing graphics processing units (GPUs) speeds up tasks such as noise filtering, normal estimation, and surface reconstruction by parallelizing calculations at the hardware level, which enables real-time or near-real-time processing (Dong et al., 2022; Jakob et al., 2021); (3) data reduction methods such as adaptive down-sampling help reduce computational burden while preserving critical structural features. For instance, uniform grid sampling selectively reduces point density in non-critical regions and preserves higher resolution in deformation-sensitive areas for accurate structural analysis (Gurram et al., 2013; Wang et al., 2021).

6.2. Challenges of point cloud noise and data incompleteness

Point clouds captured in tunnel environments are often affected by noise, redundancy, and data gaps, which pose significant challenges for accurate geometric analysis, deformation monitoring, and defect detection. These issues arise from the complexity of tunnel environments, including confined spaces, irregular surfaces, reflective materials, and adverse environmental factors (Bao et al., 2024). The presence of noise and missing data degrade point-cloud quality and increase both preprocessing complexity and the risk of analytical errors. Traditional single-threaded methods frequently struggle to efficiently handle these issues, especially in dealing with large-scale datasets or attempting real-time analysis.

(1) Sources of noise and data incompleteness

Several factors contribute to noise and data gaps in tunnel point clouds: (1) Tunnel surface materials such as metallic linings, tiles, or glossy surfaces cause irregular laser beam scattering or specular reflections, leading to noise artifacts or spurious outliers. In contrast, absorptive surfaces, such as unpolished concrete, may generate weak or missing returns, resulting in sparse regions with insufficient point cloud density. (2) Environmental factors such as dust, high humidity, and temperature fluctuations can distort laser returns, causing signal

attenuation and various measurement artifacts. These issues become more pronounced during long-term monitoring, when environmental conditions change over time. (3) Obstructive elements such as pipes, cables, and machinery, combined with the confined geometry of tunnels, prevent full surface coverage and lead to shadow regions and gaps in the point cloud. (4) Overlapping datasets acquired from multiple scan stations may introduce redundant points and misalignment errors, especially when alignment precision is insufficient.

To mitigate these challenges, a range of advanced filtering and preprocessing strategies have been proposed. Noise reduction techniques, such as statistical outlier removal, radius-based filtering, and ML-based adaptive filters, can mitigate reflection-based noise while retaining structural details (Bae et al., 2023; Xie et al., 2017). Region-specific down-sampling in less critical areas such as flat tunnel walls reduces data volume without compromising structural details, optimizing storage and processing efficiency. Leveraging GPU-based parallel processing frameworks accelerates the preprocessing stage, enabling real-time analysis more feasible even with large datasets (Li et al., 2019).

(2) Addressing data incompleteness

Incomplete regions within point-cloud data, particularly those caused by occlusions or scanning constraints, require targeted reconstruction methods to improve data continuity and accuracy. Surface reconstruction algorithms, such as delaunay triangulation, Poisson surface reconstruction, or radial basis function (RBF) interpolation, estimate missing geometry based on neighboring point distribution (Miao et al., 2019; Zeng et al., 2022). While effective for minor gaps, these methods may struggle with extensive missing areas. Integrating data from multiple scan stations or LS systems can mitigate occlusions and enhance coverage. Precise registration techniques, such as ICP or NDT, are critical for aligning and merging multi-view data into a unified point cloud (He et al., 2020; Zhang et al., 2024b). Incorporating data from complementary sensors, such as photogrammetry or infrared cameras, can provide additional information to fill gaps in the LS point cloud, enhancing overall completeness and reliability.

6.3. Challenges in high-precision point cloud registration

High-precision point cloud registration is a fundamental prerequisite for reliable tunnel deformation monitoring and defect detection. Laser scanning technology and registration algorithms have achieved substantial progress, as discussed in Section 4.1. Despite these advances, robust and high-precision registration in tunnel environments remains challenging due to the following factors:

(1) Complex tunnel geometry

Tunnels are typically characterized by repetitive and symmetrical geometric patterns, such as circular, elliptical, or horseshoe-shaped cross-sections. While advantageous for structural integrity and construction, such symmetry reduces the availability of distinctive geometric features required for unambiguous point cloud alignment. This lack of asymmetry significantly increases the risk of registration drift or false convergence. Furthermore, shield tunnels exhibit geometric irregularities, such as bends, inclines, junctions, or deformations, which exacerbate the difficulty of establishing reliable correspondences, particularly in areas where geometric features are sparse or distorted.

(2) Insufficient overlap between point clouds

Effective registration depends on sufficient overlap between adjacent scans, which enables the identification of common features across different scan stations. However, insufficient overlap often occurs due to suboptimal spacing or placement of scanning stations. Low overlap reduces the number of shared features available for alignment, impairing both the accuracy and robustness of registration algorithms. Additionally, occlusions caused by tunnel infrastructure components, such as equipment, pipes, or temporary obstacles, further limit overlap regions and increase blind spots, thereby increasing registration errors. These issues are especially prevalent in cluttered or narrow tunnel segments, where scanner maneuverability is constrained.

(3) Noise and outliers

Tunnel environments introduce various sources of noise and outliers that adversely affect the accuracy of registration algorithms. Environmental factors such as dust, high humidity, and insufficient illumination degrade point-cloud quality and interfere with reliable feature extraction. In addition, dynamic interferences caused by moving objects, including construction equipment and personnel, generate transient outliers that disrupt alignment procedures and lead to inconsistent registration results.

(4) Algorithmic limitations

Most state-of-the-art registration algorithms, such as ICP and its variants, are highly sensitive to initial conditions. However, tunnel often lack distinctive reference features, leading to frequent misalignments. In multi-station scanning, small misalignments from individual scan stations can accumulate over long distances, resulting in cumulative errors that degrade overall accuracy. Additionally, large-scale, high-density TLS or MLS point clouds demand significant computational resources, making rapid or high-precision registration computationally expensive.

(5) Feature scarcity on uniform surfaces

Tunnels often have smooth and uniform surfaces, such as concrete linings, that lack prominent features for alignment. Feature-based registration methods struggle in these scenarios due to the absence of distinctive points, lines, or surfaces that can serve as reliable reference features. To address this limitation, alternative approaches such as external reference systems or control points are often required. However, these methods can be labor-intensive and are not always feasible in long or inaccessible tunnel sections.

6.4. Challenges in multi-sensor data fusion

In tunnel monitoring applications, multi-sensor data fusion, integrating data from LS, IMUs, and cameras, is crucial for acquiring a comprehensive understanding of structural behavior and environmental conditions. Each sensor contributes unique and complementary information: LS captures high-resolution geometric data, IMUs provide motion and orientation measurements, and cameras provide detailed visual and texture information. However, multi-sensor data fusion faces significant technical challenges, arising from disparities in spatial and temporal resolution, coordinate frameworks, and sensor-specific distortions.

One of the primary challenges in multi-sensor data fusion is achieving precise spatial alignment. Each sensor operates within its own coordinate system and must transform into a common reference frame (Wang et al., 2024a). For instance, LS generates 3D point clouds in a scanner-specific frame, IMUs operate in a body-fixed system, and cameras produce 2D images in a pixel-based frame. Differences in sensor placement and calibration errors complicate this alignment process, and the absence of direct geometric correspondences between datasets further increases its difficulty. Furthermore, field-of-view mismatches between sensors exacerbate alignment difficulties. While LS scanners often capture a 360-degree environment, cameras typically focus on specific directions, and IMUs provide no spatial data. This disparity is especially problematic in tunnel environments, where visual and geometric references may be limited.

Temporal synchronization is another critical issue, as sensors typically operate at different sampling rates. LS often generates data at 100 kHz-3 MHz (for different types of laser scanning systems), while cameras capture frames at 30-60 Hz, and IMUs can reach frequencies up to 1000 Hz. Aligning these data requires interpolation or extrapolation techniques, which are vulnerable to errors if timestamps are inconsistent or inaccurate. Additionally, sensor clocks may drift over time, leading to latency and misalignment in data streams. This issue is particularly pronounced in IMUs, where accumulated drift errors can significantly impact the accuracy of fusion over extended periods.

Sensor-specific distortions further complicate multi-sensor data fusion. LS data acquired from moving platforms may contain motion-induced distortions and may also be degraded by environmental influences such as dust, moisture, or reflective surfaces, which introduce noise and missing measurements. Cameras, on the other hand, are affected by lens distortions and variable lighting conditions that can degrade image quality. IMUs, while providing essential motion data, are prone to noise and biases, and they cannot independently determine absolute positions or orientations. Correcting these distortions is a necessary prerequisite for effective fusion (Wu et al., 2022).

The integration process faces significant challenges, particularly in establishing correspondences between heterogeneous data. Aligning 3D LS points with 2D camera pixels, for example, requires precise calibration and projection, which is computationally intensive. Errors introduced by any individual sensor tend to propagate during fusion and exacerbate inaccuracies in the integrated dataset. For instance, drift in IMU motion estimates can result in incorrect trajectory corrections for LS data, while misaligned LS and camera datasets can lead to errors in texture mapping. Furthermore, the computational demands of real-time fusion, particularly for high-resolution or high-frequency data, present additional obstacles. Achieving a balance between computational efficiency and fusion accuracy remains a significant challenge.

Addressing these challenges requires a combination of strategies. Robust calibration procedures are essential to correct intrinsic distortions in individual sensors and to establish accurate spatial relationships between them. Synchronization methods, such as GPS-based timestamps or hardware trigger signals, can help align sensor clocks and reduce temporal inconsistencies. Advanced fusion algorithms, including feature-based approaches, probabilistic models, and DL techniques, show promise in improving robustness and accuracy, particularly in noisy environments. Motion-induced distortions can be mitigated using IMU data for correction, while computational optimization through parallel processing or hardware accelerators such as GPUs can enhance the feasibility of real-time fusion (Li et al., 2019).

In conclusion, while multi-sensor data fusion holds considerable potential advantages for tunnel monitoring, it involves complex challenges that require meticulous calibration, synchronization, and algorithmic development, as described in Table 8. By addressing these issues, it is possible to achieve high-precision fusion that enables comprehensive and reliable deformation monitoring and defect detection in challenging tunnel environments.

7. Future trends and developments of LS in shield tunnel monitoring

7.1. Technological innovations in LS for shield tunnel monitoring

The application of LS in shield tunnel monitoring has witnessed substantial advancements over the years, with significant progress in both hardware technologies and data processing methodologies. These developments enhance the precision, efficiency, and reliability of tunnel maintenance and long-term infrastructure monitoring. This section highlights two primary trends: hardware innovation and the integration of multi-source data.

7.1.1. Hardware advancements

The evolution of LS hardware continues to enhance its applicability in shield tunnel monitoring. Modern LS sensors are becoming

Table 8
A summary of existing challenges in LS data processing and potential solutions.

Challenge type	Technical gaps	Manifestations of challenges	Existing limitations	Solving strategies
Large-Scale Data Processing	– High deployment cost; – High hardware expense.	Data storage and management	– Massive data volume; – Limited scalability; – Difficult storage management.	– Utilization of distributed storage systems such as HDFS (Ahmed et al., 2023); – Advanced data compression algorithms, such as Octree (Qin et al., 2024) and Voxel Grid (Lyu et al., 2024).
		Computational challenges in processing large datasets	– Low computational efficiency; – Insufficient capability of processing environment.	– Parallel and distributed computing frameworks such as Apache Spark (Paredes et al., 2024) and Google Cloud Dataflow (Akidau et al., 2021); – GPU acceleration; – Adaptive down-sampling (Gurram et al., 2013; Wang et al., 2021).
Point Cloud Noise and Incomplete Data	– Cumulative errors multi-station stitching; – Poor surface reconstruction.	Noise and data incompleteness	– Noise influences; – Data gaps; – Redundancy and misalignment from multiple scan stations.	Utilization of advanced filtering and preprocessing strategies; – Noise reduction techniques, such as statistical outlier removal, radius-based filtering, and ML-based adaptive filters (Bae and Kim, 2023; Xie and Lu, 2017).
		Data incompleteness	– Occlusions or scanning constraints.	– Surface reconstruction algorithms; – Precise registration techniques (He et al., 2020; Zhang et al., 2024b); – Incorporating data of multi-sensors.
High-Precision Point Cloud Registration	– Suboptimal spacing or placement of scanning stations; – Difficulties of target placement; – Environmental noise; – Dynamic interference.	Complex tunnel geometry Insufficient overlap Noise and outliers Algorithmic limitations Feature scarcity	– Geometric irregularities of real-world tunnels. – Suboptimal spacing or placement of scanning stations. – Inevitable noise existence in laser scanning data. – Highly sensitive to initial conditions and data quality. – Risks of registration drift or false convergence for the lack of asymmetry.	
Multi-Sensor Data Fusion	– Lack of direct geometric correspondences between datasets; – Field-of-view mismatches.	Differences between multi-sensor data	– Limited spatial and temporal alignment accuracy; – Cross-format correspondence challenges.	– Synchronization methods development; – Advanced fusion algorithms; – IMU data for motion-induced distortions correction (Li et al., 2019).

increasingly compact, lightweight, and energy-efficient, allowing deployment in constrained underground spaces. Recent advances in LS hardware include high-resolution systems capable of generating dense point clouds with sub-millimeter accuracy, which is essential for detecting subtle deformations or structural anomalies in tunnels. Additionally, advancements in scanning speed and range have enabled the rapid collection of high-quality data over extended distances, reducing operational downtime. Dual- and multi-wavelength LS systems are emerging, offering the potential for simultaneous measurement of different surface properties, such as reflectivity and material composition, which are critical for identifying tunnel defects like cracks, leakage, or surface erosion.

The integration of LS with robotic platforms, such as unmanned ground vehicles (UGVs) and drones (Hawley et al., 2022), further enhances its operational flexibility. These mobile platforms may support inspection in complex tunnel geometries.

7.1.2. Multi-source data integration

The fusion of LS data with information from other sensors represents a pivotal trend in shield tunnel monitoring. Combining LS point clouds with data from photogrammetry, thermal imaging, ground-penetrating radar (GPR), and IMUs facilitates a more comprehensive understanding of tunnel conditions. For example, thermal imaging can reveal temperature variations associated with leakage (Han et al., 2022; Yahia et al., 2021), while GPR can detect subsurface anomalies (Liu et al., 2023b; Peng et al., 2021), such as voids or delamination, that LS alone may not identify.

Recent advances in artificial intelligence and ML algorithms further enhance the processing and analysis of multi-source data (Sun et al., 2024; Yu et al., 2018). By integrating LS point clouds with images and other sensor data, AI-powered models can accurately classify defects, predict potential failures, and prioritize maintenance efforts. Such systems may also enable real-time monitoring and decision-making, significantly improving the responsiveness and reliability of tunnel management.

7.1.3. Future directions

Future research may focus on hybrid LS systems that integrate traditional laser scanning with emerging sensing modalities such as hyperspectral or terahertz imaging, which could enhance the characterization of tunnel surfaces. In addition, the adoption of cloud computing and edge processing technologies will streamline data management, enabling faster and more efficient analysis of increasingly large datasets.

In summary, hardware innovation and multi-source data integration are expanding the capabilities to meet the growing demands of modern infrastructure management. These trends will enable more accurate, efficient, and proactive approaches to ensure the safety and longevity of shield tunnels.

7.2. Trends in intelligent data processing for shield tunnel monitoring

The rapid advancement of ML and DL techniques is transforming the processing and analysis of LS point cloud data in shield tunnel monitoring. These intelligent methodologies offer unprecedented opportunities to extract meaningful insights from complex, high-dimensional datasets, improving the accuracy, efficiency, and automation of tunnel assessment. This section explores current trends in ML and DL applications in point cloud processing and discusses the potential role of large-scale models in advancing this field.

7.2.1. Machine learning and deep learning for point cloud processing

ML and DL have demonstrated remarkable success in addressing the challenges inherent in processing LS point clouds. Traditional approaches to tunnel monitoring often rely on manual feature extraction or heuristic algorithms, which are time-consuming and prone to errors. In contrast, ML algorithms can automatically learn complex patterns from the data, significantly enhancing defect detection and classification (Jiang et al., 2025).

DL models, including convolutional neural networks (CNNs), graph neural networks (GNNs), and point-based architectures such as PointNet and PointNet++, have revolutionized the analysis of unstructured point cloud data (Li et al., 2023; Lin et al., 2024; Yu et al., 2024). These models excel at segmenting tunnel surfaces, identifying structural anomalies, and classifying defects such as cracks, deformations, and leakages. For example, DL methods can efficiently distinguish between tunnel lining surfaces and defects, even in noisy or incomplete datasets, thereby improving reliability (Guo et al., 2024; Liu et al., 2025; Zheng et al., 2024).

Recent research also highlights the integration of DL models with time-series data to monitor the progression of tunnel defects (Chen et al., 2024a). By combining spatial and temporal information, these models can predict future structural issues, supporting timely and targeted maintenance strategies. Moreover, advances in semi-supervised and unsupervised learning can help mitigate the scarcity of labeled training data, which remains a major challenge in tunnel monitoring.

7.2.2. The potential of large models in point cloud analysis

Large-scale pre-trained models from natural language processing (e.g., GPT-style architectures) and computer vision (e.g., Vision Transformers) are beginning to influence the domain of 3D point cloud processing. Unlike traditional DL models, these models, trained on extensive datasets, exhibit exceptional zero-shot generalization capabilities across diverse tasks and domains, offering transformative potential for tunnel monitoring applications (Ling et al., 2024).

Adapting large models for point cloud data involves leveraging pre-trained backbones and employing parameter-efficient fine-tuning to capture the geometric characteristics of tunnel linings. Such models can serve as powerful feature extractors, enabling tasks like defect detection, semantic segmentation, and surface classification with minimal task-specific customization. Moreover, their ability to transfer knowledge from other domains, such as urban infrastructure or geological surveys, reduces the need for extensive labeled datasets in the tunnel monitoring context. Large models also present opportunities for integrating multi-modal data, such as combining point clouds with thermal images, videos, or SHM data. This holistic approach enhances the contextual understanding of tunnel conditions, improving the accuracy and robustness of monitoring systems (Li et al., 2025).

One emerging approach is the adoption of DeepSeek-series models, which offers a transformative trajectory for subterranean point cloud processing, driven by its computationally economic framework and advanced logical reasoning capabilities. Architecturally, the deployment of Mixture-of-Experts (MoE) sparse-computation strategies facilitates the development of high-capacity yet low-latency point-based networks, enabling the real-time processing of massive-scale tunnel datasets on edge-computing devices. Regarding task orchestration, the model's superior reasoning acts as a high-level controller that autonomously decomposes complex monitoring objectives, such as segment dislocation quantification, into standardized algorithmic sequences. Furthermore, the multimodal alignment capabilities of the DeepSeek-VL series allow for the cross-modal transfer of radiometric and textural knowledge to 3D point clouds, thereby bolstering the robustness of leakage detection and defect classification under small-sample constraints (Er et al., 2025; Gao et al., 2025). Finally, its proficiency in automated code synthesis and mathematical optimization significantly accelerates the iterative development of bespoke LS processing libraries, transitioning tunnel monitoring from labor-intensive workflows toward a highly autonomous, data-driven intelligence ecosystem.

7.2.3. Future directions in intelligent data processing

The convergence of DL models, large models, and cloud-based computing platforms represents a key direction for advancing

intelligent data processing in shield tunnel monitoring. Innovations may include: (1) Real-time processing and decision-making. With advancements in edge computing and efficient DL algorithms, real-time monitoring and analysis of tunnel conditions will become feasible, reducing response times to potential threats; (2) Explainable AI (XAI). The adoption of explainable AI techniques will provide deeper insights into the decision-making processes of ML models, enhancing their transparency and trustworthiness for critical infrastructure applications; (3) Collaborative AI models. Large-scale collaborative AI models, trained on diverse datasets from multiple infrastructure systems, could provide universal solutions adaptable to various tunnel environments and monitoring objectives.

In conclusion, intelligent data processing powered by ML models, DL models, and large models is set to revolutionize the analysis of LS point cloud data for shield tunnel monitoring. These advancements will enable more accurate, automated, and proactive tunnel management, address the growing complexity and demand of modern infrastructure systems.

8. Conclusions

Laser scanning technology has become a crucial component of deformation monitoring and defect assessment in shield tunnels due to its capability to capture high-resolution three-dimensional representations of structural conditions. This review highlights the significant advancements in LS systems, including improvements in point-cloud density and accuracy, as well as the integration of complementary sensing modalities such as IMUs and imaging devices. These advancements enable the precise detection of critical tunnel defects, such as cracks, spalling, and leakage, which are vital for early intervention and maintenance planning.

Despite these benefits, several technical challenges remain unresolved, including managing the vast volume of point cloud data, mitigating noise and data incompleteness, and achieving robust multi-sensor data fusion. High-precision registration remains particularly difficult in tunnel environments due to complex geometries, insufficient feature density, and environmental interference. Furthermore, the computational demands of real-time processing and the limited generalizability of current defect-detection methods across diverse tunnel conditions continue to pose significant challenges.

Future research should focus on developing advanced data processing algorithms, leveraging AI-based methods to enhance defect detection and streamline multi-sensor data fusion. Advances in hardware, such as lightweight and high-performance LS systems, combined with computational optimizations using GPUs and cloud-based processing frameworks, are essential to meet the growing demand for real-time monitoring. Additionally, standardizing methods for integrating LS data into existing tunnel management systems will be crucial for widespread adoption.

In conclusion, LS has already demonstrated considerable potential in tunnel monitoring. Further improvements in sensing hardware, data processing, and multi-sensor integration can enhance its overall effectiveness and support the safety, sustainability, and operational efficiency of underground infrastructure.

CRediT authorship contribution statement

Shihan Fu: Writing – original draft, Investigation, Conceptualization. **Yueqian Shen:** Writing – review & editing, Supervision, Project administration, Conceptualization. **Jinhu Wang:** Validation. **Jundi Jiang:** Writing – original draft, Investigation. **Junjun Huang:** Writing – original draft, Data curation.

Declaration of competing interest

The authors declare that they have no known competing financial interests or personal relationships that could have appeared to influence the work reported in this paper.

Acknowledgement

This work was supported by the National Natural Science Foundation of China (Grant No. 42571513).

Data availability

No data was used for the research described in the article.

References

Ahmed, M.A., Khafagy, M.H., Shaheen, M.E., Kaseb, M.R., 2023. Dynamic replication policy on HDFS based on machine learning clustering. IEEE Access 11, 18551–18559.
Aiger, D., Mitra, N.J., Cohen-Or, D., 2008. 4-points congruent sets for robust pairwise surface registration. ACM Trans. Graph. 27, 1–10.
Akidau, T., Begoli, E., Chernyak, S., Hueske, F., Knight, K., Knowles, K., Mills, D., Sotolongo, D., 2021. Watermarks in stream processing systems: Semantics and comparative analysis of Apache Flink and Google Cloud Dataflow. Proceedings of the VLDB Endowment 14, 3135–3147.
Al-Durgham, K., Habib, A., 2014. Association-matrix-based sample consensus approach for automated registration of terrestrial laser scans using linear features. Photogramm. Eng. Remote Sens. 80, 1029–1039.
Arastounia, M., 2016. Automated As-built model generation of subway tunnels from mobile LiDAR data. Sensors 16, 1486.
Attard, L., Debono, C.J., Valentino, G., Di Castro, M., 2018. Tunnel inspection using photogrammetric techniques and image processing: a review. ISPRS J. Photogramm. Remote Sens. 144, 180–188.
Bae, S.J., Kim, J.Y., 2023. Indoor clutter object removal method for an as-built building information model using a two-dimensional projection approach. Appl. Sci.-Basel 13, 9636.
Balado, J., Díaz-Vilariño, L., Arias, P., González-Jorge, H., 2018. Automatic classification of urban ground elements from mobile laser scanning data. Autom. Constr. 86, 226–239.
Bao, Y., Wen, Y.C., Tang, C., Sun, Z., Meng, X.L., Zhang, D.L., Wang, L., 2024. Three-dimensional point cloud denoising for tunnel data by combining intensity and geometry information. Sustainability 16, 2077.
Barnea, S., Filin, S., 2007. Registration of terrestrial laser scans via image based features. International Archives of Photogrammetry, Remote Sensing and Spatial Information Sciences 36, 32–37.
Bauer, P., Woschitz, H., 2024. Laboratory Investigations of the Leica RTC360 laser scanner-distance measuring performance. Sensors 24, 3742.
Beloch, L., Pavelka, K., 2024. Optimizing mobile laser scanning accuracy for urban applications: a comparison by strategy of different measured ground points. Appl. Sci.-Basel 14, 3387.
Brenner, C., Dold, C., Ripperda, N., 2008. Coarse orientation of terrestrial laser scans in urban environments. ISPRS J. Photogramm. Remote Sens. 63, 4–18.
Cabo, C., Ordóñez, C., Argüelles-Fraga, R., 2017. An algorithm for optimizing terrestrial laser scanning in tunnels. Autom. Constr. 83, 163–168.
Cao, Z., Chen, D., Shi, Y., Zhang, Z., Jin, F., Yun, T., Xu, S., Kang, Z., Zhang, L., 2019. A Flexible architecture for extracting metro tunnel cross sections from terrestrial laser scanning point clouds. Remote Sens 11, 297.
Chen, L., Tian, Z., Zhou, S., Gong, Q., Di, H., 2024a. Attitude deviation prediction of shield tunneling machine using time-aware LSTM networks. Transp. Geotech. 45, 101195.
Chen, Q., Kang, Z., Cao, Z., Xie, X., Guan, B., Pan, Y., Chang, J., 2024b. Combining cylindrical voxel and mask R-CNN for automatic detection of water leakages in shield tunnel point clouds. Remote Sens. 16.
Chen, Y.L., Shen, S.L., Zhou, A.N., 2025. Extraction of assembly quality information in shield tunnels from LiDAR data. Measurement 245, 116541.
Cheng, Y.-J., Qiu, W., Lei, J., 2016. Automatic extraction of tunnel lining cross-sections from terrestrial laser scanning point clouds. Sensors 16, 1648.
Cheng, L., Chen, S., Liu, X.Q., Xu, H., Wu, Y., Li, M.C., Chen, Y.M., 2018. Registration of laser scanning point clouds: a review. Sensors 18, 1641.
Cheng, X., Hu, X., Tan, K., Wang, L., Yang, L., 2021. Automatic detection of shield tunnel leakages based on terrestrial mobile LiDAR intensity images using deep learning. IEEE Access 9, 55300–55310.
Choo, J.-H., Park, S., Kim, D.-S., Noh, E.-C., 2024. An application of MMS in precise inspection for safety and diagnosis of road tunnel. J. Korean Tunnell. Underground Space Assoc. 26, 113–128.
Choy, C., Gwak, J., Savarese, S., 2019. 4D Spatio-Temporal ConvNets: Minkowski Convolutional Neural Networks. In: 2019 IEEE/CVF Conference on Computer Vision and Pattern Recognition (CVPR), Long Beach, CA, USA, pp. 3070–3079.
Cui, H., Ren, X., Mao, Q., Hu, Q., Wang, W., 2019. Shield subway tunnel deformation detection based on mobile laser scanning. Autom. Constr. 106, 102889.
Cui, H., Mao, Q., Li, J., Hu, Q., Tao, Y., Ma, J., Li, Z., 2024a. Shield tunnel dislocation detection method based on semantic segmentation and bolt hole positioning of MLS point cloud. IEEE Trans. Geosci. Remote Sens. 62, 5702815.

Cui, L.Z., Liu, J., Luo, H.Z., Wang, J.H., Zhang, X., Lv, G.H., Xie, Q.Y., 2024b. Deformation measurement of tunnel shotcrete liner using the Multiepoch LiDAR point clouds. J. Constr. Eng. Manag. 150, 14.
Di Stefano, F., Chiappini, S., Gorreja, A., Balestra, M., Pierdicca, R., 2021. Mobile 3D scan LiDAR: a literature review. Geomat. Nat. Haz. Risk 12, 2387–2429.
Dold, C., Brenner, C., 2004. Automatic matching of terrestrial scan data as a basis for the generation of detailed 3D city models. Int. Arch. Photogramm. Remote Sensing 35, 1091–1096.
Dong, X., Xiao, Y., Chen, Z., Yao, J., Guo, X., 2022. GPU-based supervoxel segmentation for 3D point clouds. Comput. Aided Geom. Des. 93, 102080.
Du, L., Zhong, R., Sun, H., Liu, Y., Wu, Q., 2019. Cross-section positioning based on a dynamic MLS tunnel monitoring system. Photogram. Rec. 34, 244–265.
Du, L., Zhong, R., Sun, H., Pang, Y., Mo, Y., 2022. Dislocation detection of shield tunnel based on dense cross-sectional point clouds. IEEE Trans. Intell. Transp. Syst. 23, 22227–22243.
Er, K.S., Ryozo, K., Kwan, B.H., Goh, C.H., Loo, J.L., Ng, D.-W.-K., 2025. Semantic segmentation from 3D LiDAR Data using Visual Large Language Model (VLLM). In: 2025 IEEE 6th International Conference in Robotics and Manufacturing Automation (ROMA), pp. 24–28.
Fan, S., Dong, Q., Zhu, F., Lv, Y., Ye, P., Wang, F.Y., 2021. SCF-Net: Learning Spatial Contextual Features for Large-Scale Point Cloud Segmentation. In: 2021 IEEE/CVF Conference on Computer Vision and Pattern Recognition (CVPR), pp. 14499–14508.
Fekete, S., Diederichs, M., Lato, M., 2010. Geotechnical and operational applications for 3-dimensional laser scanning in drill and blast tunnels. Tunn. Undergr. Space Technol. 25, 614–628.
Feng, S.J., Feng, Y., Zhang, X.L., Chen, Y.H., 2023. Deep learning with visual explanations for leakage defect segmentation of metro shield tunnel. Tunn. Undergr. Space Technol. 136, 105107–105125.
Gao, X., Jian, M., Hu, M., Tanniru, M., Li, S., 2019. Faster multi-defect detection system in shield tunnel using combination of FCN and faster RCNN. Adv. Struct. Eng. 22, 2907–2921.
Gao, K., Lu, D., Li, L., Chen, N., He, H., Xu, L., Li, J., 2025. Digital buildings analysis: 3-D modeling, GIS integration, and visual descriptions using gaussian splatting, ChatGPT/Deepseek, and Google Maps Platform. IEEE Geosci. Remote Sens. Lett. 22, 1–5.
Gikas, V., 2012. Three-dimensional laser scanning for geometry documentation and construction management of highway tunnels during excavation. Sensors 12, 11249–11270.
Gressin, A., Mallet, C., Demantké, J., David, N., 2013. Towards 3D lidar point cloud registration improvement using optimal neighborhood knowledge. ISPRS J. Photogramm. Remote Sens. 79, 240–251.
Guan, H., Li, J., Cao, S., Yu, Y., 2016. Use of mobile LiDAR in road information inventory: a review. Int. J. Image Data Fusion 7, 219–242.
Guo, Z., Wei, J., Sun, H., Zhong, R., Ji, C., 2024. Enhanced water leakage detection in shield tunnels based on laser scanning intensity images using RDES-Net. IEEE J. Sel. Top. Appl. Earth Obs. Remote Sens. 17, 5680–5690.
Gurram, P., Hu, S., Chan, A., 2013. Uniform Grid Upsampling of 3D LiDAR Point Cloud Data, Conference on Three-Dimensional Image Processing (3DIP) and Applications. Burlingame, CA.
Habib, A., Ghanma, M., Morgan, M., Al-Ruzouq, R., 2005. Photogrammetric and LiDAR data registration using linear features. Photogramm. Eng. Remote Sens. 71, 699–707.
Han, J.-Y., Guo, J., Jiang, Y.-S., 2013a. Monitoring tunnel deformations by means of multi-epoch dispersed 3D LiDAR point clouds: an improved approach. Tunn. Undergr. Space Technol. 38, 385–389.
Han, S., Cho, H., Kim, S., Jung, J., Heo, J., 2013b. Automated and efficient method for extraction of tunnel cross sections using terrestrial laser scanned data. J. Comput. Civ. Eng. 27, 274–281.
Han, L., Chen, J., Li, H., Liu, G., Leng, B., Ahmed, A., Zhang, Z., 2022. Multispectral water leakage detection based on a one-stage anchor-free modality fusion network for metro tunnels. Autom. Constr. 140, 104345.
Hänsch, R., Weber, T., Hellwich, O., 2014. Comparison of 3D interest point detectors and descriptors for point cloud fusion. ISPRS Ann. Photogramm. Remote Sens. Spatial Inf. Sci. 2, 57–64.
Hawley, C.J., Gräbe, P., 2022. Water leakage mapping in concrete railway tunnels using LiDAR generated point clouds. Constr. Build. Mater. 361, 129644.
He, Y., Yang, J., Li, Z.H., Liang, B., 2020. ICP Registration Base on 3D Point Clouds Feature Descriptor, 12th International Conference on Graphics and Image Processing (ICGIP). Xian, Peoples R China.
Huang, J., Liu, W., Sun, X., 2014. A pavement crack detection method combining 2D with 3D information based on Dempster-Shafer theory. Comput. Aided Civ. Inf. Eng. 29, 299–313.
Huang, H., Sun, Y., Xue, Y., Wang, F., 2017. Inspection equipment study for subway tunnel defects by grey-scale image processing. Adv. Eng. Inf. 32, 188–201.
Huang, H.-W., Li, Q.-T., Zhang, D.-M., 2018. Deep learning based image recognition for crack and leakage defects of metro shield tunnel. Tunn. Undergr. Space Technol. 77, 166–176.
Huang, H., Cheng, W., Zhou, M., Chen, J., Zhao, S., 2020. Towards automated 3D inspection of water leakages in shield tunnel linings using mobile laser scanning data. Sensors 20, 6669.
Hu, D., Li, Y., Yang, X., Liang, X., Zhang, K., Liang, X., 2023. Experiment and application of NATM tunnel deformation monitoring based on 3D laser scanning. Struct. Control Health Monit. 2023, 3341788.
Jakob, J., Guthe, M., 2021. Optimizing LBVH-Construction and Hierarchy-Traversal to accelerate *k*NN Queries on Point Clouds using the GPU. Comput. Graphics Forum 40, 124–137.
Jeong, S., Kim, M.-G., Kim, S.-T., Oh, K.-Y., 2023. Crack inspection in tunnel structures by fusing information from a 3D light detection and ranging and pan-tilt-zoom camera system. Structures 58, 105420.
Ji, A., Chew, A.W.Z., Xue, X., Zhang, L., 2022a. An encoder-decoder deep learning method for multi-class object segmentation from 3D tunnel point clouds. Autom. Constr. 137, 104187.
Ji, C., Sun, H., Zhong, R., Li, J., Han, Y., 2022b. Precise positioning method of moving laser point cloud in shield tunnel based on bolt hole extraction. Remote Sens. 14, 4791.
Jian, L., Qiu, W., Cheng, Y., 2025. Centerline-based registration for shield tunnel 3D reconstruction using spinning mid-range LiDAR point cloud and multi-cameras. Autom. Constr. 171, 105950.
Jiang, H., Li, Q., Jiao, Q., Wang, X., Wu, L., 2018. Extraction of wall cracks on earthquake-damaged buildings based on TLS point clouds. IEEE J. Sel. Top. Appl. Earth Obs. Remote Sens. 11, 3088–3096.
Jiang, J., Shen, Y., Wang, J., Wang, J., Zhang, C., Wang, J., Ferreira, V., 2025. GEPT-Net: an efficient geometry enhanced point transformer for shield tunnel leakage segmentation. ISPRS J. Photogramm. Remote Sens. 221, 20–43.
Jing, Y., Lin, W., Sheil, B., Acikgoz, S., 2025. 3D multimodal feature for infrastructure anomaly detection. Autom. Constr. 178, 106388.
Johnson, A.E., Hebert, M., 1999. Using spin images for efficient object recognition in cluttered 3D scenes. IEEE Trans. Pattern Anal. Mach. Intell. 21, 433–449.
Kang, Z., Li, J., Zhang, L., Zhao, Q., Zlatanova, S., 2009. Automatic registration of terrestrial laser scanning point clouds using panoramic reflectance images. Sensors 9, 2621–2646.
Kang, Z., Zhang, L., Tuo, L., Wang, B., Chen, J., 2014. Continuous extraction of subway tunnel cross sections based on terrestrial point clouds. Remote Sens. 6, 857–879.
Kim, J.M., Seung-Hee, H., 2022. A study on the national basic map road part renewal method using high definition map. J. Korean Soc. Geospat. Inf. Sci. 30, 3–11.
Kuang, G., Li, B., Mo, S., Hu, X., Li, L., 2022. Review on machine learning-based defect detection of shield tunnel lining. Periodica Polytechnica-Civil Engineering 66, 943–957.
Lai, Q.Y., Xin, Q.C., Tian, Y.H., Chen, X.Y., Li, Y.J., Wu, R.H., 2025. Structural analysis and 3D reconstruction of underground pipeline systems based on LiDAR point clouds. Remote Sens. 17, 341.
Lam, S.Y., 2006. Application of terrestrial laser scanning methodology in geometric tolerances analysis of tunnel structures. Tunn. Undergr. Space Technol. 21, 410.
Lee, J., Yu, K., Kim, Y., Habib, A.F., 2007. Adjustment of discrepancies between LIDAR data strips using linear features. IEEE Geosci. Remote Sens. Lett. 4, 475–479.
Li, J., Xu, Y., Macrander, H., Atkinson, L., Thomas, T., Lopez, M.A., 2019. GPU-based lightweight parallel processing toolset for LiDAR data for terrain analysis. Environ. Model. Software 117, 55–68.
Li, D., Xie, Q., Gong, X., Yu, Z., Xu, J., Sun, Y., Wang, J., 2021. Automatic defect detection of metro tunnel surfaces using a vision-based inspection system. Adv. Eng. Inf. 47, 101206.
Li, J., Zhang, Z., Sun, H., Xie, S., Zou, J., Ji, C., Lu, Y., Ren, X., Wang, L., 2023. GL-Net: Semantic segmentation for point clouds of shield tunnel via global feature learning and local feature discriminative aggregation. ISPRS J. Photogramm. Remote Sens. 199, 335–349.
Li, P., Mi, X., Ding, P., Sun, W., Zhang, H., Liu, C., Dong, Z., Yang, B., 2024. Fusion of vehicle-mounted imagery and point cloud for road boundary extraction and vectorization. Geomat. Inf. Sci. Wuhan Univ. 49, 631–639.
Li, X., Li, S., Yuan, J., Wan, Z., Liu, X., 2025. A data-driven and knowledge graph-based research on safety risk-coupled evolution analysis and assessment in shield tunneling. Tunn. Undergr. Space Technol. 162, 106657.
Liao, J., Yue, Y., Zhang, D., Tu, W., Cao, R., Zou, Q., Li, Q., 2022. Automatic tunnel crack inspection using an efficient mobile imaging module and a lightweight CNN. IEEE Trans. Intell. Transp. Syst. 23, 15190–15203.
Lin, W., Li, P., Xie, X., 2022. A novel detection and assessment method for operational defects of pipe jacking tunnel based on 3D longitudinal deformation curve: a case study. Sensors (Basel) 22, 7648.
Lin, W., Sheil, B., Zhang, P., Zhou, B., Wang, C., Xie, X., 2024. Seg2Tunnel: A hierarchical point cloud dataset and benchmarks for segmentation of segmental tunnel linings. Tunn. Undergr. Space Technol. 147, 105735.
Lin, W., Sheil, B., Zhang, P., Chang, J., Xie, X., 2025a. Automated digital reconstruction of high-fidelity present-day geometries for segmental tunnel linings based on segmented point clouds. Tunn. Undergr. Space Technol. 164, 106859.
Lin, W., Sheil, B., Zhang, P., Li, K., Xie, X., 2025b. Structural geometry-informed 3D deep learning for segmental tunnel lining analysis in point clouds. Autom. Constr. 176, 106281.
Lindenbergh, R., Pfeifer, N., Rabbani, T., 2005. Accuracy analysis of the Leica HDS3000 and feasibility of tunnel deformation monitoring. In: Proceedings of the ISPRS Workshop Laser Scanning 2005, Enschede, the Netherlands, pp. 24-29.
Ling, J., Li, X., Li, H., An, Y., Rui, Y., Shen, Y., Zhu, H., 2024. Hybrid NLP-based extraction method to develop a knowledge graph for rock tunnel support design. Adv. Eng. Inf. 62, 102725.
Liu, J., Sun, Q., Fan, Z., Jia, Y., 2018. TOF lidar development in autonomous vehicle. In: 2018 IEEE 3rd Optoelectronics Global Conference (OGC), Shenzhen, China, pp. 185–190.
Liu, S., Sun, H., Zhang, Z., Li, Y., Zhong, R., Li, J., Chen, S., 2022a. A multiscale deep feature for the instance segmentation of water leakages in tunnel using MLS point cloud intensity images. IEEE Trans. Geosci. Remote Sens. 60, 1–16.
Liu, X., Zhu, L., Wang, Y., Yu, Z., 2022b. A crack detection system of subway tunnel based on image processing. Measurement & Control 55, 164–177.

Liu, C., Liu, Y., Chen, Y., Zhao, C., Qiu, J., Wu, D., Liu, T., Fan, H., Qin, Y., Tang, K., 2023a. A state-of-the-practice review of three-dimensional laser scanning technology for tunnel distress monitoring. J. Perform. Constr. Facil 37, 03123001.
Liu, H., Yue, Y., Lai, S., Meng, X., Du, Y., Cui, J., Spencer, B.F., 2023b. Evaluation of the antenna parameters for inspection of hidden defects behind a reinforced shield tunnel using GPR. Tunn. Undergr. Space Technol. 140, 105265.
Liu, Z.Y., Gao, X.J., Yang, Y.W., Xu, L., Wang, S.N., Chen, N.S., Wang, Z.W., Kou, Y., 2025. EDT-Net: a lightweight tunnel water leakage detection network based on LiDAR point clouds intensity images. IEEE J. Sel. Top. Appl. Earth Obs. Remote Sens. 18, 7334–7346.
Lu, Z., Zhu, F., Shi, L., Wang, F., Zeng, P., Hu, J., Liu, X., Xu, Y., Chen, Q., 2019. Automatic seepage detection in cable tunnels using infrared thermography. Meas. Sci. Technol. 30, 115902.
Lyu, W., Ke, W., Sheng, H., Ma, X., Zhang, H.Y., 2024. Dynamic downsampling algorithm for 3D point cloud map based on voxel filtering. Appl. Sci.-Basel 14, 16.
Ma, L., Li, Y., Li, J., Wang, C., Wang, R., Chapman, M.A., 2018. Mobile laser scanned point-clouds for road object detection and extraction: a review. Remote Sens. 10, 1531.
Miao, W., Liu, Y., Shi, X., Feng, J., Xue, K., 2019. A 3D surface reconstruction method based on Delaunay triangulation. In: Image and Graphics: 10th International Conference, ICIG 2019, Beijing, China, pp. 40-51.
Monserrat, O., Crosetto, M., 2008. Deformation measurement using terrestrial laser scanning data and least squares 3D surface matching. ISPRS J. Photogramm. Remote Sens. 63, 142–154.
Mukupa, W., Roberts, G.W., Hancock, C.M., Al-Manasir, K., 2017. A review of the use of terrestrial laser scanning application for change detection and deformation monitoring of structures. Surv. Rev. 49, 99–116.
Murakami, T., Saito, N., Komachi, Y., Michikawa, T., Sakashita, M., Kogure, S., Kase, K., Wada, S., Midorikawa, K., 2018. High spatial resolution LIDAR for detection of cracks on tunnel surfaces. In: Conference on Lasers and Electro-Optics (CLEO), San Jose, CA, USA, paper ATu3I.6.
Paredes, D.T., López, M.A., Buján, S., Richter, R., Döllner, J., 2024. Multistage strategy for ground point filtering on large-scale datasets. J. Supercomput. 80, 25974–26001.
Pejić, M., 2013. Design and optimisation of laser scanning for tunnels geometry inspection. Tunn. Undergr. Space Technol. 37, 199–206.
Peng, M., Wang, D., Liu, L., Shi, Z., Shen, J., Ma, F., 2021. Recent advances in the GPR detection of grouting defects behind shield tunnel segments. Remote Sens. 13, 4596.
Puente, I., Akinci, B., González-Jorge, H., Díaz-Vilariño, L., Arias, P., 2016. A semi-automated method for extracting vertical clearance and cross sections in tunnels using mobile LiDAR data. Tunn. Undergr. Space Technol. 59, 48–54.
Qian, J., Xue, F., Wang, T., Lin, Z., Cai, M., Shou, F., 2025. Combining SfM and deep learning to construct 3D point cloud models of shield tunnels and Realize spatial localization of water leakages. Measurement 250, 117114.
Qin, T., Li, G., Gao, W., Liu, S., 2024. Multi-grained point cloud geometry compression via dual-model prediction with extended octree. ACM Trans. Multimed. Comput. Commun. Appl. 20, 1–30.
Rashidi, M., Mohammadi, M., Sadeghlou Kivi, S., Abdolvand, M.M., Truong-Hong, L., Samali, B., 2020. A decade of modern bridge monitoring using terrestrial laser scanning: review and future directions. Remote Sens. 12, 3796.
Reulke, R., Wehr, A., Griesbach, D., 2004. Mobile panoramic mapping using CCD-line camera and laser scanner with integrated position and orientation system. In: Dagstuhl Seminar on Imaging beyond the Pinhole Camera. Springer, p. 165.
Roca-Pardiñas, J., Argüelles-Fraga, R., de Asís López, F., Ordóñez, C., 2014. Analysis of the influence of range and angle of incidence of terrestrial laser scanning measurements on tunnel inspection. Tunn. Undergr. Space Technol. 43, 133–139.
Rusu, R.B., Blodow, N., Beetz, M., 2009. Fast point feature histograms (FPFH) for 3D registration. In: 2009 IEEE International Conference on Robotics and Automation (ICRA), Kobe, Japan, pp. 3212–3217.
Sanchiz-Viel, N., Bretagne, E., Mouaddib, E.M., Dassonvalle, P., 2021. Radiometric correction of laser scanning intensity data applied for terrestrial laser scanning. ISPRS J. Photogramm. Remote Sens. 172, 1–16.
Savitzky, A., Golay, M.J.E., 1964. Smoothing and differentiation of data by simplified least squares procedures. Anal. Chem. 36, 1627–1639.
Shen, N., Wang, B., Ma, H.Y., Zhao, X., Zhou, Y., Zhang, Z.X., Xu, J.H., 2023. A review of terrestrial laser scanning (TLS)-based technologies for deformation monitoring in engineering. Measurement 223, 113684.
Shen, Y., Huang, J., Wang, J., Jiang, J., Li, J., Ferreira, V., 2024. A review and future directions of techniques for extracting powerlines and pylons from LiDAR point clouds. Int. J. Appl. Earth Obs. Geoinf. 132, 104056.
Shen, S.-L., Zhang, J.-X., Chen, Y.-L., Zhou, A., 2025. Identification of segment joint and automatic segmentation for shield tunnel based on LiDAR detection. Tunn. Undergr. Space Technol. 163, 106758.
Shokri, D., Rastiveis, H., Sheikholeslami, S.M., Shahhoseini, R., Li, J., 2021. Fast extraction of power lines from mobile LiDAR point clouds based on SVM classification in non-urban area. Earth Observ. Geomat. Eng. 5, 63–73.
Soudarissanane, S., Lindenbergh, R., Menenti, M., Teunissen, P., 2009. Incidence angle influence on the quality of terrestrial laser scanning points. In: Proceedings of the ISPRS Workshop Laser Scanning 2009, Paris, France, pp. 183–188.
Sun, H., Liu, S., Zhong, R., Du, L., 2020a. Cross-section deformation analysis and visualization of shield tunnel based on mobile tunnel monitoring system. Sensors 20, 1006.
Sun, H., Xu, Z., Yao, L., Zhong, R., Du, L., Wu, H., 2020b. Tunnel monitoring and measuring system using mobile laser scanning: Design and deployment. Remote Sens. 12, 730.
Sun, J.L., Zhang, R.F., Du, S., Zhang, L.Q., Liu, Y., 2020c. Global adaptive 4-points congruent sets registration for 3D indoor scenes with robust estimation. IEEE Access 8, 7539–7548.
Sun, W., Wang, J., Jin, F., Li, Y., Yang, Y., 2022. An adaptive cross-section extraction algorithm for deformation analysis. Tunnelling Underground Space Technol 121, 104332.
Sun, M., Xu, X., Zhou, D., Li, J., He, X., 2024. Synchronous acquisition control system and coordinate correction algorithm for subway tunnel comprehensive detection equipment. IEEE Sens 25, 1440–1451.
Taheri, H., Xia, Z.C., 2021. SLAM; definition and evolution. Eng. Appl. Artif. Intel. 97, 25.
Tan, K., Cheng, X., Ju, Q., Wu, S., 2016. Correction of mobile TLS intensity data for water leakage spots detection in metro tunnels. IEEE Geosci. Remote Sens. Lett. 13, 1711–1715.
Tang, L., He, J., Peng, W., Huang, H., Chen, C., Yu, C., 2023. Assessing the visibility of urban greenery using MLS LiDAR data. Landsc. Urban Plan. 232, 104662.
Van Gosliga, R., Lindenbergh, R., Pfeifer, N., 2006. Deformation analysis of a bored tunnel by means of terrestrial laser scanning. In: Proceedings of the ISPRS Commission V Symposium “Image Engineering and Vision Metrology”, Dresden, Germany, pp. 167–172.
Von Hansen, W., Gross, H., Thoennessen, U., 2008. Line-based registration of terrestrial and airborne LIDAR data. In: The International Archives of the Photogrammetry, Remote Sensing and Spatial Information Sciences, 37, pp. 161–166.
Wang, Z., Brenner, C., 2008. Point based registration of terrestrial laser data using intensity and geometry features. Int. Arch. Photogrammetry, Remote Sens. Spat. Inf. Sci. 37, 583–590.
Wang, H.C., Feng, D.M., 2024. Rapid geometric evaluation of transportation infrastructure based on a proposed low-cost portable mobile laser scanning system. Sensors 24, 425.
Wang, B., Kang, Z., 2012. Self-closure global registration for subway tunnel point clouds. In: 2012 International Conference on Computer Vision in Remote Sensing. IEEE, pp. 152–157.
Wang, W., Zhao, W., Huang, L., Vimarlund, V., Wang, Z., 2014. Applications of terrestrial laser scanning for tunnels: a review. J. Traffic Transp. Eng. 1, 325–337.
Wang, W., Chen, W., Wang, K., Li, S., 2020. Extraction of tunnel center line and cross-sections on fractional calculus, 3D invariant moments and best-fit ellipse. Opt. Laser Technol. 128, 106220.
Wang, J.Q., Fan, Y.G., Li, G.S., Yu, D.F., 2021. Adaptive point cloud reduction based on multi-parameter k-means clustering. Laser & Optoelectronics Progress 58, 0610008.
Wang, A., Togo, R., Ogawa, T., Haseyama, M., 2022a. Defect Detection of Subway Tunnels Using Advanced U-Net Network. Sensors 22, 2330.
Wang, K., Wu, X., Li, H., Wang, F., Zhang, L., Chen, H., 2022b. Adaptively unsupervised seepage detection in tunnels from 3D point clouds. Struct. Infrastruct. Eng. 1–19.
Wang, K., Zhang, Z., Wu, X., Zhang, L., 2022c. Multi-class object detection in tunnels from 3D point clouds: an auto-optimized lazy learning approach. Adv. Eng. Inf. 52, 101543.
Wang, L., Wang, S., You, Z., 2024b. Spatially Connected Component Analysis Based 3d Detection and Visualization of Subway Tunnel Lining Water Leakage Using Mls Data. Available at SSRN 4892163.
Williams, K., Olsen, M.J., Roe, G.V., Glennie, C., 2013. Synthesis of transportation applications of mobile LiDAR. Remote Sens. 5, 4652–4692.
Wu, H., Ao, X., Chen, Z., Liu, C., Xu, Z., Yu, P., 2019. Concrete spalling detection for metro tunnel from point cloud based on roughness descriptor. Journal of Sensors 2019, 8574750.
Wu, Q.X., Meng, Q.Y., Tian, Y.Y., Zhou, Z.R., Luo, C.F., Mao, W.D., Zeng, P.L., Zhang, B. T., Luo, Y.B., 2022. A method of calibration for the distortion of LiDAR integrating IMU and odometer. Sensors 22, 6716.
Xie, X., Lu, X., 2017. Development of a 3D modeling algorithm for tunnel deformation monitoring based on terrestrial laser scanning. Underground Space 2, 16–29.
Xie, X., Tian, H., Zhou, B., Li, K., 2021. The life-cycle development and cause analysis of large diameter shield tunnel convergence in soft soil area. Tunn. Undergr. Space Technol. 107, 103680.
Xu, S., Wang, R., 2019. Power line extraction from mobile LiDAR point clouds. IEEE J. Sel. Top. Appl. Earth Obs. Remote Sens. 12, 734–743.
Xu, X., Yang, H., 2019. Intelligent crack extraction and analysis for tunnel structures with terrestrial laser scanning measurement. Adv. Mech. Eng. 11 (9), 1–7.
Xu, T., Xu, L., Li, X., Yao, J., 2018a. Detection of water leakage in underground tunnels using corrected intensity data and 3D point cloud of terrestrial laser scanning. IEEE Access 6, 32471–32480.
Xu, X., Yang, H., Neumann, I., 2018b. A feature extraction method for deformation analysis of large-scale composite structures based on TLS measurement. Compos. Struct. 184, 591–596.
Xu, Y., Li, D., Xie, Q., Wu, Q., Wang, J., 2021. Automatic defect detection and segmentation of tunnel surface using modified Mask R-CNN. Measurement 178, 109316.
Xu, L., Gong, J., Na, J., Yang, Y., Tan, Z., Pfeifer, N., Zheng, S., 2022. Shield tunnel convergence diameter detection based on self-driven mobile laser scanning. Remote Sens. 14, 767.
Xue, Y., Li, Y., 2018. A fast detection method via region-based fully convolutional neural networks for shield tunnel lining defects. Comput. Aided Civ. Inf. Eng. 33, 638–654.
Xue, Y., Shi, P., Jia, F., Huang, H., 2022. 3D reconstruction and automatic leakage defect quantification of metro tunnel based on SfM-Deep learning method. Underground Space 7, 311–323.
Yahia, M., Gawai, R., Ali, T., Mortula, M.M., Albasha, L., Landolsi, T., 2021. Non-destructive water leak detection using multitemporal infrared thermography. IEEE Access 9, 72556–72567.

Yang, H., Xu, X., 2020. Intelligent crack extraction based on terrestrial laser scanning measurement. Measurement & Control 53, 416–426.
Yang, B., Zang, Y., Dong, Z., Huang, R., 2015. An automated method to register airborne and terrestrial laser scanning point clouds. ISPRS J. Photogramm. Remote Sens. 109, 62–76.
Yang, J., Wang, C., Luo, W., Zhang, Y., Chang, B., Wu, M., 2021. Research on point cloud registering method of tunneling roadway based on 3D NDT-ICP algorithm. Sensors 21, 4448.
Yi, C., Lu, D., Xie, Q., Liu, S., Li, H., Wei, M., Wang, J., 2019. Hierarchical tunnel modeling from 3D raw LiDAR point cloud. Comput. Aided Des. 114, 143–154.
Yi, C., Lu, D., Xie, Q., Xu, J., Wang, J., 2020. Tunnel deformation inspection via global spatial axis extraction from 3D raw point cloud. Sensors 20, 6815.
Yin, Z., Lei, Z., Zheng, A., Zhu, J., Liu, X.-Z., 2023. Automatic detection and association analysis of multiple surface defects on shield subway tunnels. Sensors 23, 7106.
You, Z., Wang, L., 2025. Dislocation detection of shield tunnel segments under non-uniform deformation conditions using RMLS point clouds. ISPRS Ann. Photogramm. Remote Sens. Spatial Inf. Sci. X-1/W2-2025, 195–204.
Yu, A., Mei, W., 2024. Deep-learning-based longitudinal joint opening detection method for metro shield tunnel. Tunn. Undergr. Space Technol. 154, 106108.
Yu, Y., Li, J., Guan, H., Wang, C., 2014. 3D crack skeleton extraction from mobile LiDAR point clouds. In: 2014 IEEE Geoscience and Remote Sensing Symposium. IEEE, pp. 914–917.
Yu, P., Wu, H., Liu, C., Xu, Z., 2018. Water leakage diagnosis in metro tunnels by intergration of laser point cloud and infrared thermal imaging. Int. Arch. Photogramm. Remote. Sens. Spat. Inf. Sci. 42, 2167–2171.
Yu, A., Mei, W., Han, M., 2021. Deep learning based method of longitudinal dislocation detection for metro shield tunnel segment. Tunn. Undergr. Space Technol. 113, 103949.
Yu, J., Lv, D., Tian, M., Zhang, Y., Lin, J., Xu, F., Shi, G., 2022. Automatic extraction of tunnel centerline and cross-sections from 3D point clouds. Eng. Res. Express 4, 015026.
Yue, Z., Sun, H., Zhong, R., Du, L., 2021. Method for tunnel displacements calculation based on mobile tunnel monitoring system. Sensors 21, 4407.
Zeng, Y.J., Zhu, Y.P., 2022. Implicit surface reconstruction based on a new interpolation/approximation radial basis function. Comput. Aided Geom. Des. 92, 19.
Zhang, W., Zhang, Z., Qi, D., Liu, Y., 2014. Automatic crack detection and classification method for subway tunnel safety monitoring. Sensors 14, 19307–19328.
Zhang, W., Qiu, W., Song, D., Xie, B., 2019. Automatic tunnel steel arches extraction algorithm based on 3D LiDAR point cloud. Sensors 19, 3972.
Zhang, Z., Ji, K., Dang, J., 2021. Research on an image-based crack detection method for subway tunnels based on feature analysis. J. Electron. Imaging 30, 053020.
Zhang, Z., Ji, A., Wang, K., Zhang, L., 2022. UnrollingNet: an attention-based deep learning approach for the segmentation of large-scale point clouds of tunnels. Autom. Constr. 142, 104456.
Zhang, Z., Ji, A., Zhang, L., Xu, Y., Zhou, Q., 2023. Deep learning for large-scale point cloud segmentation in tunnels considering causal inference. Autom. Constr. 152, 104915.
Zhang, C., Chen, X., Liu, P., He, B., Li, W., Song, T., 2024a. Automated detection and segmentation of tunnel defects and objects using YOLOv8-CM. Tunn. Undergr. Space Technol. 150, 105857.
Zhang, J.R., Xie, F.F., Sun, L., Zhang, P., Zhang, Z.P., Chen, J.P., Chen, F.R., Yi, M.Z., 2024b. Multi-view point cloud registration based on improved NDT algorithm and ODM optimization method. IEEE Rob. Autom. Lett. 9, 6816–6823.
Zheng, A., Qi, S.M., Cheng, Y.Q., Wu, D., Zhu, J.S., 2024. Efficient detection of apparent defects in subway tunnel linings based on deep learning methods. Appl. Sci.-Basel 14, 7824.
Zhou, M., Cheng, W., Huang, H., Chen, J., 2021. A Novel Approach to Automated 3D Spalling Defects Inspection in Railway Tunnel Linings Using Laser Intensity and Depth Information. Sensors 21, 5725.
Zhou, H., Gao, B., Wu, W., 2023. Automatic crack detection and quantification for tunnel lining surface from 3D terrestrial LiDAR data. J. Eng. Res. 11, 239–257.
Zhu, H., Jin, J., Zhao, S., 2025. Research on multi-sensor data fusion based real-scene 3D reconstruction and digital twin visualization methodology for coal mine tunnels. Sensors 25, 6153.